

**TRANSCRIPTOME META-ANALYSIS OF MOUSE LENSES DEFICIENT
FOR KEY GENES TO UNCOVER REGULATORY PATHWAYS IN LENS
DEVELOPMENT AND PATHOLOGY**

by

Sarah Yacoba Coomson

A thesis submitted to the Faculty of the University of Delaware in partial fulfillment of the requirements for the degree of Master of Science in Bioinformatics and Computational Biology

Summer 2025

© 2025 Sarah Yacoba Coomson
All Rights Reserved

**TRANSCRIPTOME META-ANALYSIS OF MOUSE LENSES DEFICIENT
FOR KEY GENES TO UNCOVER REGULATORY PATHWAYS IN LENS
DEVELOPMENT AND PATHOLOGY**

by

Sarah Yacoba Coomson

Approved: _____
Salil A. Lachke, Ph.D.
Professor in charge of thesis on behalf of the Advisory Committee

Approved: _____
Cathy Wu, Ph.D.
Director of the Center for Bioinformatics & Computational Biology

Approved: _____
Caleb Everett, Ph.D.
Dean of the College of Arts and Sciences

Approved: _____
Louis F. Rossi, Ph.D.
Vice Provost for Graduate and Professional Education and
Dean of the Graduate College

ACKNOWLEDGMENTS

I would like to express my deepest gratitude to my advisor, Dr. Salil A. Lachke, for encouraging me to embark on this journey and for his unwavering support throughout the process. His guidance, mentorship, and understanding have been instrumental in shaping both this work and my growth as a scientist. I am truly thankful for the direction he has provided and the confidence he has placed in me.

I am also sincerely grateful to my committee members, Dr. Abhyudai Singh and Dr. Shawn Polson, for their time, thoughtful feedback, and continued support. I deeply appreciate their kindness, insightful suggestions, and willingness to accommodate my needs despite their busy schedules. Special thanks to the faculty members in the Bioinformatics and Computational Biology program who have generously shared their knowledge and skills. Their teaching has significantly enriched my academic experience and prepared me for this research. I am especially thankful to Ms. Amelia Harrison, Ms. Heather Justison, and Dr. Karen Hooper for their exceptional administrative support. Their consistent assistance made navigating the logistics of graduate school far more manageable.

I extend heartfelt thanks to my family. To my parents, whose sacrifices made it possible for me to be here, and to my sisters, who have supported me both financially and emotionally. I am also thankful to my wider community, whose encouragement, motivation, and belief in me have carried me through difficult moments.

Above all, I give thanks to God for His grace, strength, and faithfulness throughout this journey.

TABLE OF CONTENTS

LIST OF TABLES	vi
LIST OF FIGURES	vii
ABSTRACT	x

Chapter

1	INTRODUCTION	1
1.1	Overview of the ocular Lens	1
1.2	Regulation of lens development	3
1.3	Cataract and other lens developmental defects	8
1.4	Transcriptomic studies in lens biology	12
1.5	iSyTE	13
1.6	Aims, objectives and motivation for this study	14
2	MATERIALS AND METHODS	16
2.1	Data Collection	16
2.2	Quality Control and Preprocessing	17
2.3	Read Alignment	17
2.4	Gene Expression Quantification	18
2.5	Differential Expression Analysis	18
2.6	Functional Enrichment Analysis	19
2.7	Data Visualization	19
2.8	Statistical Analysis	19
3	RESULTS	20
3.1	Clustering of embryonic control samples reveals developmental stage-specific patterns	20
3.2	Differential expression analysis across embryonic lens cKO datasets	22
3.3	Lens expression profiles of top differentially expressed genes	25
3.4	Gene ontology enrichment reveals functional disruption of lens-specific processes in embryonic KO lenses	30
3.5	GO enrichment analysis of 31 high-confidence DEGs highlights lens-specific functions	34

3.6	Early postnatal lens control samples cluster according to developmental stage and similar gene expression profiles	35
3.7	Differential expression analysis reveals limited but targeted misregulation across early postnatal cKOs	38
3.8	GO analysis of upregulated genes reveals abnormal retinal gene expression in early postnatal KO lens	44
3.9	Functional categorization of downregulated genes in early postnatal lens KOs	44
3.10	Clustering of Adult Control Lens Samples	46
3.11	Differential expression analysis identifies widespread transcriptomic changes in adult lens Kos	46
3.12	Gene ontology enrichment analysis of differentially expressed genes in adult lens KOs	48
4	DISCUSSION.....	52
5	FUTURE DIRECTIONS.....	57
	REFERENCES.....	58

LIST OF TABLES

Table 1.1 Lens knockout RNA-seq datasets used in this meta-analysis study.....	17
Table 3.1 Differentially expressed genes between embryonic KO and control lens samples using unadjusted p-value < 0.05.....	22
Table 3.2 Differentially expressed genes using adjusted p-value < 0.05.....	22
Table 3.3 Top 20 upregulated genes in embryonic lens KO samples	26
Table 3.4. Top 20 downregulated genes in embryonic lens KO samples	28
Table 3.5 Differentially expressed genes between early postnatal lens cKO and controls using unadjusted p-value < 0.05.....	38
Table 3.6 List of 13 upregulated DEGs in early postnatal lens KOs	40
Table 3.7 List of 23 downregulated DEGs in early postnatal lens KOs.....	41
Table 3.8 Gene Ontology (BP) analysis of upregulated genes in early postnatal KO lenses	45
Table 3.9 Gene Ontology (CC) analysis of upregulated genes in early postnatal KO lenses	45

LIST OF FIGURES

- Figure 1.1 Schematic representation of the mammalian eye. The anterior segment comprises the cornea and lens, which contribute to light refraction, while the posterior segment contains the retina, responsible for photoreception and image processing (Dash et al., 2016)..... 2
- Figure 1.2. Lens development in mice. At E9.5, optic vesicle (OV) becomes closely associated with overlying head surface ectoderm thereby inducing lens placode (LP) formation. LP and OV then invaginate coordinately to form the lens pit (LPT) which goes on to form the lens vesicle (LV) and optic cup (OC) respectively. OC contributes to the retina (RT) and LV develops into the lens which has an anterior epithelium (AE) and primary fibers (PF) in the posterior region. AE cells differentiate into secondary fiber cells (FC) at the transition zone throughout life. Modified from Kuszak & Brown (1994)..... 4
- Figure 1.3. Gene regulatory network of early mammalian lens development. Signals and activity of transcription factors from the optic vesicle initiate a gene regulatory cascade in the pre-lens ectoderm, leading to lens placode formation. Figure from Lachke and Maas 2010. 6
- Figure 1.4. Post-transcriptional regulation of gene expression by RNA-binding proteins (RBPs). RBPs recognize and bind specific sequence and structural motifs within target mRNAs and regulate key stages of the mRNA lifecycle, including 5' capping, splicing, 3' polyadenylation, nuclear export, cytoplasmic localization, stability and translation. Figure from Lachke 2022. 7
- Figure 1.5. Loss of lens transparency is termed cataract. In normal lens (left), light entering the eye is focused sharply onto the retina for clear vision. In a cataractous lens (right), light is scattered and not focused properly onto the retina hence the individual perceives a blurry image. 9
- Figure 1.7. Microphthalmia and Anophthalmia. (a) Bilateral anophthalmia characterized by complete absence of both eyes. (b) Bilateral microphthalmia showing severely reduced sizes in both eyes. (c) Unilateral anophthalmia with complete absence of one eye and presence of a false eye (white asterisk). Figure from Harding & Moosajee, 2019 11

Figure 3.1 Clustering of embryonic lens control samples based on transcriptomic profiles. (A) Heatmap of the top 500 most variable genes across embryonic lens control samples from multiple RNA-seq datasets, showing hierarchical clustering by developmental stage. (B) Principal Component Analysis (PCA) plot in two dimensions showing separation of control samples by developmental stage. (C) 3-Dimensional PCA plot illustrating enhanced separation of control samples. Each point represents one biological replicate; colors indicate developmental stage.....	21
Figure 3.2 Differential expression analysis of embryonic lens KO samples versus controls. MA plot showing average log expression (x-axis) versus log ₂ fold change (y-axis) across all embryonic samples. Red points indicate significantly upregulated genes; blue points indicate downregulated genes (Log ₂ FC ≥ 0.58 , p-value < 0.05).	23
Figure 3.3 Volcano plot of differentially expressed genes in embryonic lens KO samples. Log ₂ fold change versus -log ₁₀ p-value. Red and blue dots represent significantly upregulated and downregulated genes, respectively (log ₂ FC ≥ 0.58 , p-value < 0.05). Labeled genes represent top 40 DEGs.	24
Figure 3.4. iSyTE expression and enriched expression profile of the top 20 upregulated genes in embryonic lens KO samples. Heatmap showing expression (A) and enriched expression (B) of the top upregulated DEGs in mouse lens stages. Note: Not all 20 genes were found in the iSyTE database; the heatmap includes only those with available data ...	27
Figure 3.5. iSyTE expression profile of the top 20 downregulated genes in embryonic lens KO samples. Heatmap of downregulated DEGs showing high expression (A) and strong lens enrichment (B) during embryonic development, consistent with roles in lens structure and function. Note: Only genes with available expression data in iSyTE are shown.....	29
Figure 3.6 Gene Ontology enrichment dot plots for all DEGs in embryonic lens cKO samples (A) Cellular Component (CC) terms enriched in DEGs. (B) Biological Process (BP) terms enriched in DEGs, (C) Molecular Function (MF) terms enriched in DEGs.....	31
Figure 3.7 GO enrichment dot plots for upregulated and down regulated DEGs in embryonic KO lenses. (A) BP terms for upregulated genes. (B) MF terms for upregulated genes. (C) BP terms for downregulated genes (D) MF terms for downregulated genes	33

Figure 3.8 Gene Ontology analysis of the 31 DEGs identified using FDR cutoff (adjusted p-value < 0.05) across embryonic lens cKO datasets. GO analysis was performed using DAVID, and enriched terms are shown across the three categories.	35
Figure 3.9 Clustering analysis of early postnatal lens control samples.(A) Heatmap of the top 500 most variable genes across early postnatal control samples.(B) 3-D PCA plot showing spatial separation of control samples.	37
Figure 3.10 Volcano plot of differentially expressed genes in early postnatal lens cKO samples. All 36 DEGs are labelled	39
Figure 3.11 iSyTE analysis of upregulated DEGs from early postnatal KO lenses (A) Expression and (B) lens enrichment patterns for upregulated DEGs across mouse lens developmental stages.	42
Figure 3.12 iSyTE analysis of downregulated DEGs from early postnatal KO lenses (A) Expression and (B) lens enrichment patterns for downregulated DEGs across mouse lens developmental stages.	43
Figure 3.13 Clustering of adult lens control samples by 3-D PCA plot.	46
Figure 3.14 Volcano plot of DEGs in adult KO lenses. Log2 fold change versus – log10 p-value. Red and blue dots represent significantly upregulated and downregulated genes, respectively ($\log_2FC \geq 0.58 $, p-value < 0.05). Labeled genes represent top 40 DEGs	47
Figure 3.15 iSyTE analysis of upregulated DEGs from adult KO lenses (A) Expression and (B) lens enrichment patterns for upregulated DEGs across mouse lens developmental stages.	49
Figure 3.16 iSyTE analysis of downregulated DEGs from adult KO lenses (A) Expression and (B) lens enrichment patterns for downregulated DEGs across mouse lens developmental stages.	50
Figure 3.17 GO enrichment dot plots for upregulated and down regulated DEGs. (A) BP terms for upregulated genes. (B) MF terms for upregulated genes. (C) BP terms for downregulated genes (D) MF terms for downregulated genes	51

ABSTRACT

The vertebrate lens is a powerful model to study tissue-specific gene regulation, development, and disease. Recent advances in high-throughput transcriptomics have yielded a growing number of high-throughput RNA-sequencing (RNA-seq) datasets from knockout (KO) and mutant mouse models carrying deletion/mutations of specific genes essential for lens biology and perturbations of which are linked to cataract in humans or animal models. However, these studies are often analyzed in isolation, limiting the discovery of shared regulatory programs and broader biological insights. A systematic meta-analysis of these RNA-seq datasets has not been performed, representing a key knowledge-gap. Therefore, I performed a comprehensive meta-analysis of publicly available lens KO RNA-seq datasets – which spanned embryonic, early postnatal, and adult stages – to identify common transcriptional programs and misregulated pathways relevant to lens biology. Raw FASTQ files were downloaded from the NCBI Gene Expression Omnibus (GEO) using SRR accession numbers and processed through an elaborate pipeline. Normalization was conducted using edgeR, with meta-analysis performed separately for embryonic, early postnatal, and adult datasets. Gene Ontology (GO) enrichment was assessed using enrichGO (clusterProfiler) and Database for Annotation, Visualization and Integrated Discovery (DAVID), and lens-specific expression and enrichment were evaluated using the web-based eye bioinformatics tool, iSyTE (integrated Systems Tool for Eye gene discovery). This analysis led, for the first time, to the identification of a cohort of genes that are commonly mis-expressed in the lens, regardless of the specific gene perturbation. Thus,

this analysis identified a set of genes whose mis-regulation correlates with lens pathology. In embryonic datasets, differentially expressed genes (DEGs) were highly enriched for processes central to lens morphogenesis, such as lens fiber cell differentiation, and visual system development. Many downregulated genes, including *Crygf*, *Crygb*, *Dnase2b*, and *Bfsp1* – identified in the present analysis – are known for their critical role in facilitating lens transparency, serving as an independent validation of the meta-analysis having worked well for the identification of key genes in the lens. Besides the established, novel genes whose function is not yet characterized in the lens were also identified (*Tmprss11e*, *Ermap*, *Uox*). In early postnatal datasets, a smaller set of DEGs was identified, including ectopically upregulated retinal genes (*Prph2*, *Pdc*, *Pde6b*). In adult lenses, a novel gene *Ces5a* was identified as significantly downregulated in the knockout samples. In wild-type (WT) lenses, *Ces5a* shows moderate expression during development and early postnatal stages, but its expression increases sharply—by over 17-fold—by postnatal day 56 (P56), where it exhibits a 26-fold enrichment compared to whole-body expression levels. This work provides the first stage-stratified meta-analysis of lens cKO RNA-seq data, uncovering shared and unique transcriptional consequences of gene disruption in lens development. Importantly, it identifies a set of genes whose misexpression correlates with lens pathology, regardless of the genetic changes that caused it, thus potentially identifying new targets that may be commonly targeted in therapeutic approaches.

Chapter 1

INTRODUCTION

1.1 Overview of the ocular Lens

The vertebrate eye is a highly specialized multicomponent sensory organ responsible for visual perception, with the lens situated in the anterior segment. (Graw, 2010) (Figure 1.1). The vertebrate ocular lens is a transparent, avascular tissue that together with the cornea forms a converging optical unit responsible for refracting and focusing incoming light onto the retina, thereby enabling sharp visual perception (Land, 2012). The lens is composed of two primary cell types, namely, a monolayer of anterior epithelial cells and elongated fiber cells, which constitute the bulk of the lens (Cvekl & Zhang, 2017; Lachke & Maas, 2010). During early ocular development, the lens originates from the lens placode, which invaginates to form the lens pit and subsequently the lens vesicle. As the vesicle forms, anterior cells retain their epithelial identity, while posterior cells elongate and undergo terminal differentiation into primary lens fiber cells (McAvoy et al., 1999) (Figure 1.2). Unlike most tissues, the lens continues to grow throughout life via the addition of new secondary fiber cells at its periphery. This process is sustained by lens epithelial cells located in the “germinative zone”, which actively proliferate. As these cells migrate toward the lens equatorial region, known as the transition zone, they exit the cell cycle and initiate differentiation into secondary fiber cells (Bhat, 2001). These newly formed fiber cells elongate and become tightly packed, concentric layers which create the unique architecture of the lens required for its transparency (Kuszak et al., 2004). In addition to the maintenance of this highly

ordered secondary fiber cell architecture, the functional integrity of the lens depends on lifelong transparency, both of which are essential for precise light refraction and visual clarity. Furthermore, the lens preserves its transparency by eliminating organelles in mature fiber cells to minimize light scattering and by densely packing high concentrations of crystallin proteins, which contribute to its refractive properties (Bassnett, 2002; Slingsby et al., 2013). The lens also has gap junction proteins which facilitate intercellular communications and ensures metabolic homeostasis across this avascular tissue (Mathias et al., 2010). Normal lens physiology and functionality depend on tightly regulated gene expression and signaling pathways during lens development and throughout life. Disruption of these regulatory mechanisms through genetic mutations, elevated oxidative stress, or aberrant gene expression can compromise protein stability, disrupt cellular organization, and increase light scattering, and impair lens transparency and refractive properties, ultimately resulting in cataract formation and other lens defects.

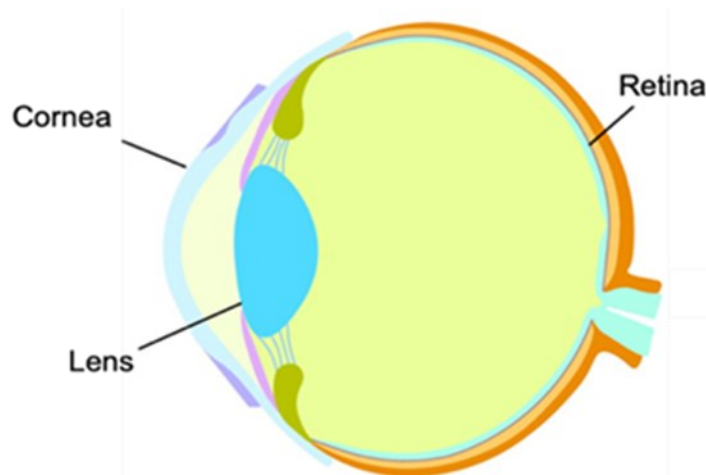


Figure 1.1 Schematic representation of the mammalian eye. The anterior segment comprises the cornea and lens, which contribute to light refraction, while the posterior segment contains the retina, responsible for photoreception and image processing (Dash et al., 2016)

1.2 Regulation of lens development

Lens development is governed by a coordinated interplay of signaling pathways, transcription factors, RNA-binding proteins (RBPs) and structural proteins that together regulate cell fate specification, differentiation, and cellular organization. These processes are precisely orchestrated during embryogenesis and remain tightly regulated throughout life to ensure proper lens formation and the long-term maintenance of transparency. Lens induction requires the concerted activity of key transcription factors, including Pax6, Six3, and Sox2, along with signaling pathways such as Bone Morphogenetic Protein (BMP) and retinoic acid (RA), which together regulate the expression of genes essential for lens cell specification and early morphogenesis (Faber et al., 2002; Liu et al., 2006; Smith et al., 2009). A schematic detailing the gene regulatory network that integrates the signaling pathways and transcription factors orchestrating early lens induction is shown in Figure 1.3 (Lachke & Maas, 2010). As lens development progresses, transcription factors such as Pax6 and Foxe3 are critical for specifying the lens epithelium and regulating the proliferation and early differentiation of lens epithelial cells (Blixt et al., 2007; Cvekl & Zhang, 2017). They also control the expression of key adhesion molecules like E-cadherin, which maintains epithelial integrity through cell-cell adhesion and cytoskeletal anchoring (Pontoriero et al., 2009). Primary fiber cell differentiation is driven by a precisely regulated gradient of fibroblast growth factor (FGF) signaling, which initiates the elongation and maturation of posterior cells in the lens vesicle (Coomson & Lachke, 2025; Robinson, 2006). In contrast, secondary fiber cell differentiation and elongation relies on the coordinated activity of transcription factors such as the Maf family members (e.g., c-Maf, Mafg), Prox1, and Hsf4 (Fujimoto et al., 2004; Patel et al., 2022; Wigle et al., 1999). Particularly, these transcription factors drive the high-level expression of

crystallin genes, which are indispensable for establishing the lens' characteristic high refractive index and maintaining transparency (Fujimoto et al., 2004; Kim et al., 1999; Yang et al., 2006).

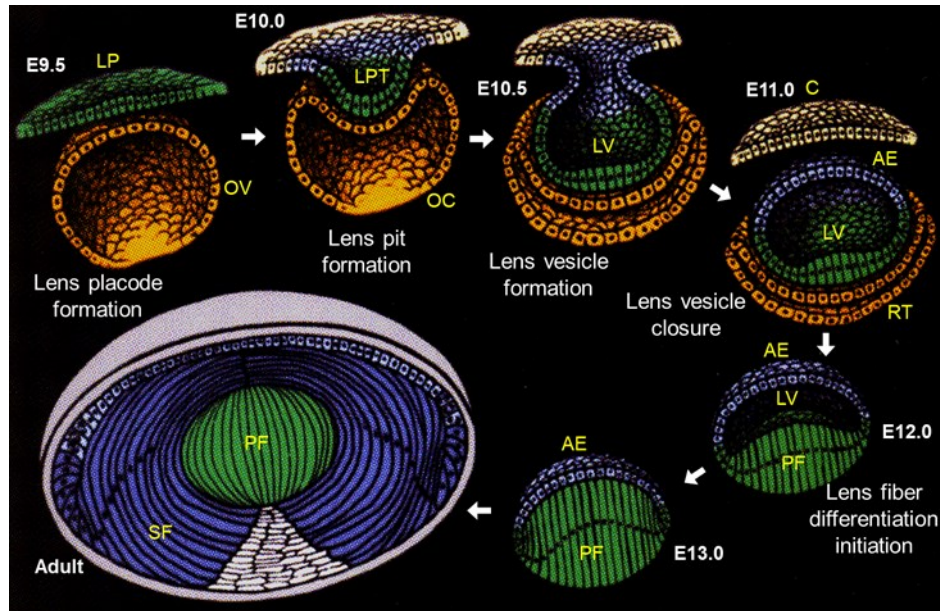


Figure 1.2. Lens development in mice. At E9.5, optic vesicle (OV) becomes closely associated with overlying head surface ectoderm thereby inducing lens placode (LP) formation. LP and OV then invaginate coordinately to form the lens pit (LPT) which goes on to form the lens vesicle (LV) and optic cup (OC) respectively. OC contributes to the retina (RT) and LV develops into the lens which has an anterior epithelium (AE) and primary fibers (PF) in the posterior region. AE cells differentiate into secondary fiber cells (FC) at the transition zone throughout life. Modified from Kuszak & Brown (1994)

Crystallins, particularly the α -, β -, and γ -crystallin families, are the major structural proteins of the lens, comprising nearly 90% of its total protein content (Wistow, 2012). While functioning to provide optical clarity and a high refractive index, crystallins function as molecular chaperones that preserve protein solubility under cellular stress (Horwitz, 2003; Klemenz et al., 1991). Moreover, cytoskeletal

components like the highly lens-enriched Bfsp1 and Bfsp2 (Perng et al., 2007), along with membrane proteins such as connexins (Gja3 and Gja8), are critical for maintaining the structure of fiber cells and facilitating intercellular communication (Gong et al., 2007; Mathias et al., 2010). The proper spatiotemporal expression of these components is necessary to preserve the lens microenvironment and support its physiological function. Notably, gene expression in the lens is dynamic and stage-specific, coordinating key processes including cell proliferation, migration, elongation, and organelle degradation during fiber cell differentiation (Disatham et al., 2019; Rao, 2008).

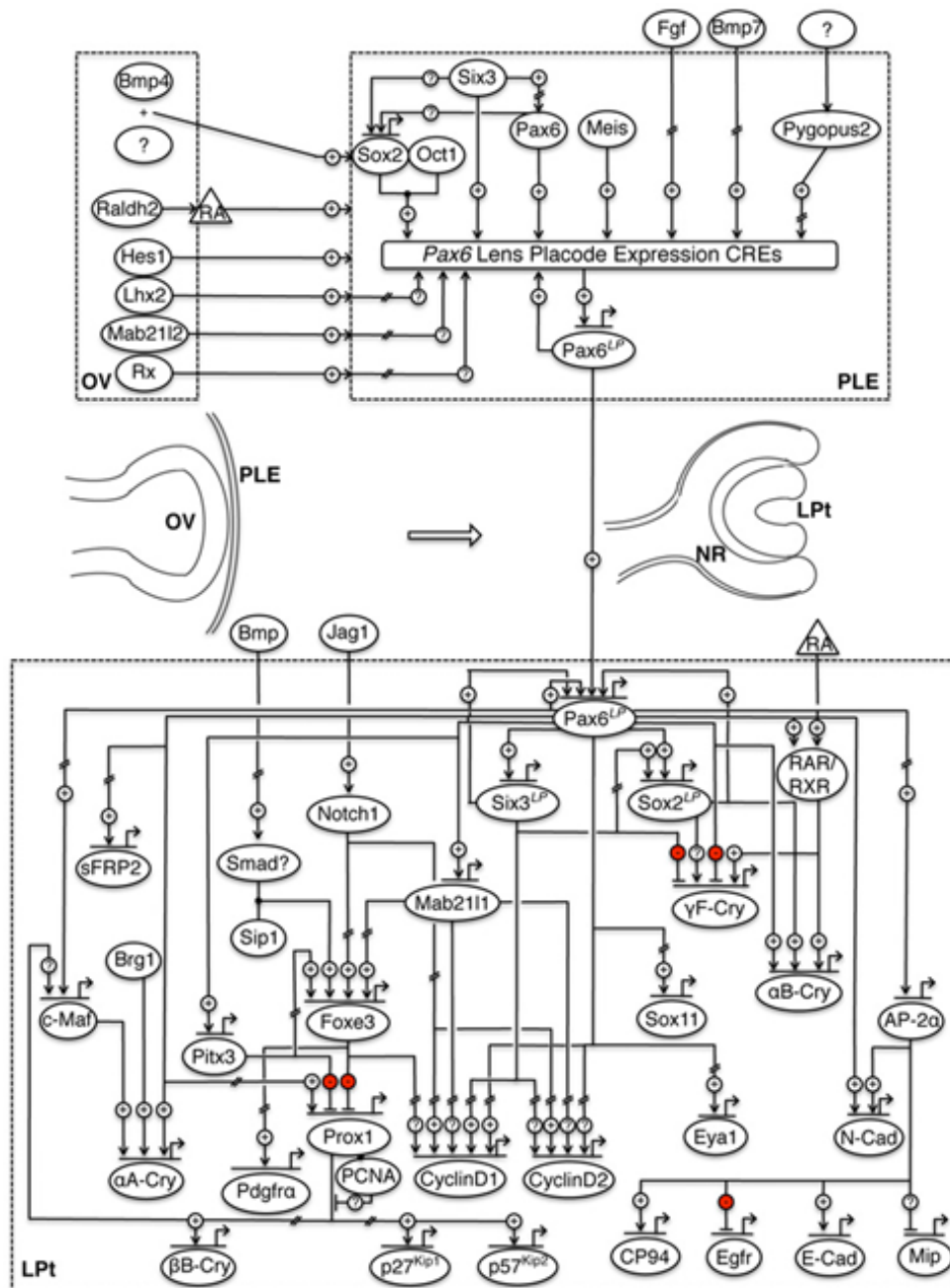


Figure 1.3. Gene regulatory network of early mammalian lens development. Signals and activity of transcription factors from the optic vesicle initiate a gene regulatory cascade in the pre-lens ectoderm, leading to lens placode formation. Figure from Lachke and Maas 2010.

In addition to signaling and transcriptional regulation, post-transcriptional control is crucial in regulating gene expression during lens development and maintaining lens homeostasis. Post-transcriptional control in the lens may be mediated by RNA-binding proteins (RBPs) (Dash et al., 2016) and non-coding RNAs such as microRNAs (miRNAs) (Yu et al., 2017). Specific RBPs recognize and bind specific sequences and structural motifs within their target mRNAs and regulate distinct events in the lifecycle of the mRNA including 5'-capping, splicing, 3'-polyadenylation, nuclear export, cytoplasmic localization, mRNA stability or decay, and translation (Figure 1.4) (Lachke, 2022). Through these diverse mechanisms, RBPs exert control over the spatial and temporal expression of proteins, ultimately shaping the cellular proteome required for proper lens structure, function, and long-term transparency (Dash et al., 2015, 2020a; Lachke et al., 2011; Siddam et al., 2018).

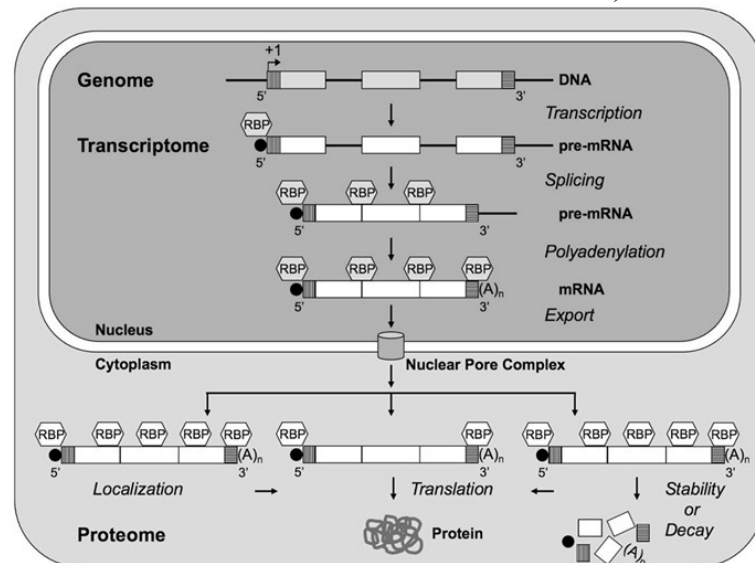


Figure 1.4. Post-transcriptional regulation of gene expression by RNA-binding proteins (RBPs). RBPs recognize and bind specific sequence and structural motifs within target mRNAs and regulate key stages of the mRNA lifecycle, including 5' capping, splicing, 3' polyadenylation, nuclear export, cytoplasmic localization, stability and translation. Figure from Lachke 2022.

Mutations or dysregulation in the expression of key signaling molecules, transcription factors, RBPs, and structural proteins in the lens have been associated with a range of ocular defects, including congenital and age-related cataracts (Lachke, 2022; Shiels & Hejtmancik, 2021). The specific timing of gene function during development is critical because the stage at which these factors are required often determines the onset and severity of the lens phenotype when they are disrupted. For instance, mutations affecting early-expressed regulatory genes frequently result in congenital cataracts, whereas alterations in genes involved in lens maintenance and homeostasis are more often linked to age-related cataract formation (Hejtmancik & Kantorow, 2004). These findings underscore the importance of precisely regulated gene expression across developmental and postnatal stages to preserve lens transparency and visual acuity.

1.3 Cataract and other lens developmental defects

Mutations in lens-specific or lens-enriched genes can disrupt developmental processes and compromise lens integrity, resulting in a range of ocular defects (Dash et al., 2020b; Rong et al., 2002). These include cataracts and aphakia, and in some cases, broader eye malformations such as microphthalmia and anophthalmia. Cataract is the opacification of the lens leading to loss of transparency resulting in reduced vision (Figure 5). Cataract is the leading cause of blindness worldwide affecting an estimated 94 million people as of 2022 (Cicinelli et al., 2023). It is primarily caused by the aggregation of destabilized lens structural proteins and crystallins which disrupt the highly ordered architecture of lens fiber cells (Moreau & King, 2012). As a result, light is scattered rather than sharply focused on the retina, impairing vision and potentially leading to complete blindness in advanced cases. Cataracts are classified by age of onset into congenital/pediatric and age-related types (Shiels & Hejtmancik, 2017). Age-related

cataract is influenced by both environmental factors and a genetic predisposition (Shiels & Hejtmancik, 2021). As one ages, even under normal conditions, crystallins in the lens fiber cells are destabilized due to cumulative oxidative stress, ultraviolet radiation, and mechanical or chemical insults (Moreau & King, 2012; Sharma & Santhoshkumar, 2009). This contributes to protein misfolding and aggregation which may lead to cataract (Moreau & King, 2012). Additionally, systemic conditions such as diabetes and myotonic dystrophy can exacerbate protein instability, further increasing cataract risk (Ivanescu et al., 2024; Moshirfar et al., 2022; Pollreis & Schmidt-Erfurth, 2010).

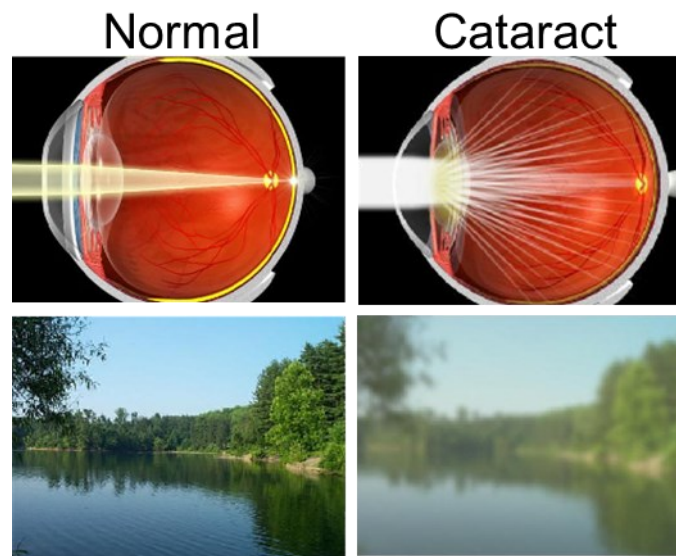


Figure 1.5. Loss of lens transparency is termed cataract. In normal lens (left), light entering the eye is focused sharply onto the retina for clear vision. In a cataractous lens (right), light is scattered and not focused properly onto the retina hence the individual perceives a blurry image.

Lens opacity present at birth is termed congenital cataract. It accounts for up to 20% of childhood blindness worldwide (Gupta et al., 2025). While their etiology is diverse, more than half of cases have a genetic basis involving mutations in genes encoding

crystallins, connexins, key structural proteins, or key transcriptional regulators of lens development (Shiels et al., 2010). Other causes include environmental factors such as prenatal viral infections (e.g., Rubella virus infection), trauma, radiation exposure and certain medications taken during pregnancy (Khokhar et al., 2018; Li et al., 2020). Congenital cataracts may occur in isolation (primary congenital cataract) or in association with other ocular diseases, genetic syndromes or even as part of systemic metabolic diseases (Bell et al., 2020). Currently, the only treatment for cataract is through surgery to replace the clouded lens with an artificial intraocular lens to restore clear vision.

More severe developmental anomalies such as microphthalmia (abnormally small eye) and anophthalmia (complete absence of the eye) affect approximately 1 in 7,000 and 1 in 30,000 live births, respectively (Harding & Moosajee, 2019). These may affect one eye (unilateral) or both eyes (bilateral) (Figure 6). Microphthalmia is often associated with other ocular abnormalities such as coloboma (missing eye tissue parts) or cataract (Harding & Moosajee, 2019). While some cases result from environmental factors such as maternal vitamin A deficiency, radiation exposure, or congenital infections, the majority are associated with complex genetic and chromosomal abnormalities (Smets et al., 2006; Verma & Fitzpatrick, 2007; Williamson & FitzPatrick, 2014). Many implicated genes associated encode transcription factors essential for early eye field specification and morphogenesis (*e.g.* Sox2, Pax6, Rax, Otx2 and Six3) and components of the retinoic acid signaling pathway, including STRA6, ALDH1A3 and RAR β (Harding & Moosajee, 2019; Williamson & FitzPatrick, 2014). Although the precise pathogenesis remains unknown, mutations in these genes may cause anophthalmia/microphthalmia through arrest of development at the optic

vesicle formation stage, lens induction failure (mediated by Sox2 and Pax6 mutations) and failure of retinal differentiation (Otx2, Chx10 and Rax mutations) (Shah et al., 2012). Importantly, defects in lens development and distinct tissues of the eye can impact overall eye size and structure. For instance, microphthalmia may arise secondary to lens malformations such as aphakia (complete absence of the lens) or lens hypoplasia (Valleix et al., 2006). In such cases, the absence or improper formation of the lens interferes with the growth cues required for normal ocular development. Other lens defects include reduced lens size and refractive errors stemming from altered morphology or protein composition, further illustrating the central role of the lens in coordinating eye development and maintaining visual function.



Figure 1.7. Microphthalmia and Anophthalmia. (a) Bilateral anophthalmia characterized by complete absence of both eyes. (b) Bilateral microphthalmia showing severely reduced sizes in both eyes. (c) Unilateral anophthalmia with complete absence of one eye and presence of a false eye (white asterisk). Figure from Harding & Moosajee, 2019

Given that genetic mutations causing cataract and other lens defects disrupt development of the tissue at various stages, it is crucial to identify the genes that regulate both lens morphogenesis and the maintenance of lens homeostasis. Elucidating these genetic regulators will advance our understanding of the molecular mechanisms underlying lens pathogenesis, representing a critical step toward identifying genetic predispositions and informing the development of targeted therapeutic strategies. Toward this, many research groups utilize mouse models and employ conditional knockout (cKO) strategies that allow specific gene deletion in the lens alone. This targeted approach enables researchers to assess specific gene function in the lens by examining phenotypic outcomes at the morphological, molecular, and cellular levels. Importantly, cKO models circumvent systemic effects associated with germline deletions, thereby enabling precise spatial and temporal dissection of lens-autonomous gene functions without confounding influences from other tissues.

1.4 Transcriptomic studies in lens biology

Over the past two decades, transcriptomic technologies such as microarrays and RNA sequencing (RNA-seq) have significantly advanced our understanding of the molecular mechanisms underlying lens development and disease. These approaches have enabled the systematic profiling of gene expression across developmental stages, comparison of healthy and diseased lenses, and evaluation of molecular consequences following specific gene knockouts in the lens. Numerous RNA-seq datasets from these lens-specific cKO models have been published, each providing valuable insight into gene-specific functions in the lens. With the growing wealth of these datasets, a logical and timely next step is to integrate them through meta-analysis to assess broader patterns or shared downstream pathways affected by multiple perturbations. Such integration can

reveal shared downstream pathways and broader regulatory patterns that may be overlooked in individual studies and reveal common pathways/mechanisms that underlie lens development and pathology. Transcriptomic datasets from wild-type (WT) lenses have been used to develop iSyTE (integrated Systems Tool for Eye gene discovery) (Kakrana et al., 2018; Lachke et al., 2012), which has supported the discovery of novel genes and pathways involved in lens development and cataractogenesis. Meta-analysis of these KO datasets holds great potential to further refine and expand iSyTE, enabling more comprehensive and systems-level insights into lens biology.

1.5 iSyTE

The integrated Systems Tool for Eye gene discovery (iSyTE) is a web-based bioinformatics resource which is designed to facilitate the identification and prioritization of genes relevant to lens development and disease. It hosts a curated collection of gene expression data from mouse eye tissues, including microarray and RNA-seq datasets at various timepoints. iSyTE utilizes lens-enrichment scores and visualization tools to enable users to identify genes with preferential expression in the lens, thereby aiding candidate gene discovery for conditions such as congenital cataracts and other lens developmental defects (Kakrana et al., 2018; Lachke et al., 2012). In recent years, iSyTE has been expanded to incorporate proteomic datasets, further enhancing its utility (Aryal et al., 2020). Leveraging iSyTE, several research groups have successfully identified and characterized genes critical for lens development and pathology (Dash et al., 2020; Siddam et al., 2018). Currently, many of iSyTE's datasets are derived from wild-type and limited knockout lens models, the latter are based only on microarray-based transcript profiles. However, none of the RNA-seq datasets from

diverse lens cKO models are currently represented in iSyTE. Incorporating these datasets would significantly broaden iSyTE's scope and analytical capabilities. Moreover, integrating meta-analyzed RNA-seq data from a wide range of lens KO models would enhance the platform's power to uncover shared regulatory mechanisms and provide a more comprehensive view of gene function and dysfunction in lens biology.

1.6 Aims, objectives and motivation for this study

Although numerous RNA-seq datasets from lens-specific KO mouse models are publicly available, no comprehensive effort has yet been made to systematically integrate and analyze these resources. Key connections between these datasets remain unexplored and limit our understanding of common misregulated pathways in lens development and disease. Therefore, a meta-analysis approach which overcomes batch effects and dataset-specific noise, is necessary to identify common gene expression signatures and regulatory pathways involved in lens pathology. This integrative approach will also provide the opportunity to distinguish universal mechanisms from gene-specific effects and offer insights that are more broadly applicable across models and potentially relevant to human disease. This study will also allow researchers to draw connections between distinct models and to formulate overarching hypotheses about lens development and pathology. By addressing this gap, the present study aims to generate a high-confidence set of differentially expressed genes and enriched pathways that are consistently affected in lens cKO models, advancing basic lens biology.

The specific objectives of this study are to:

1. Collect and preprocess publicly available RNA-seq datasets from lens-specific cKO mouse models across different developmental stages.

2. Perform quality control, read trimming, read alignment, and gene counting.
3. Conduct differential expression analysis and meta-analysis to identify conserved gene expression changes across models.
4. Perform gene ontology and pathway enrichment analysis to uncover shared biological processes and molecular mechanisms.
5. Upload the integrated results to the iSyTE platform to enhance its coverage and utility for the vision research community.

Chapter 2

MATERIALS AND METHODS

2.1 Data Collection

Publicly available RNA-Seq datasets from lens-specific conditional gene knockout mouse models were obtained from NCBI Gene Expression Omnibus (GEO) database. A systematic search was performed using keywords such as "lens conditional knockout," "mouse RNA-Seq," and gene-specific terms relevant to the study. Datasets were selected based on the availability of raw sequencing data (FASTQ files) to ensure uniform processing and standardized downstream analysis. The raw sequencing data files were downloaded from the Sequence Read Archive (SRA) using the SRA Toolkit (version 2.11.3). Specifically, the "prefetch" and "fastq-dump" commands were used to retrieve the data and convert the downloaded SRA files into FASTQ format while preserving read quality. Each dataset included both knockout and control samples, identified by their respective SRR accession numbers. This study analyzed lens RNA-Seq datasets from 13 distinct gene knockouts, namely *Atf4*, *Celf1*, *Cryaa*, *Cryab*, *Fnl1*, *Gata3*, *Itgb1*, *Mafg/Mafk*, *mir-26*, *N-myc*, *S100A4*, *Tdrd7*, and *Zeb2/Sip*. Detailed information on each dataset, including the age of the mouse lens, targeted gene, Sequencing platform, lab/research group, knockout strategy, cre type, GEO accession number and PubMed Identifier for publications (PMID) is provided in Table 1.1.

Table 1.1 Lens knockout RNA-seq datasets used in this meta-analysis study

Age	Gene KO	Platform	Lab	Knockout strategy	GEO Accession	PMID
E13.5	<i>Prox1</i> cKO	Bulk RNA-Seq	Duncan	MLR10cre	GSE69940	26657765
E14.5	<i>N-myc</i> cKO	Bulk RNA-Seq	Martins	MLR10cre	GSE94061	28716713
E14.5	<i>Gata3</i> cKO	Bulk RNA-Seq	Cvekl	Pax6-Cre	GSE131291	31847788
E15.5	<i>Zeb2/Sip1</i> cKO	Bulk RNA-Seq	Duncan	MLR10cre	GSE49949	24161570
E16.5	<i>Mafg/Mafk</i> dKO	Bulk RNA-Seq	Lachke	Germline KO	GSE207853	36092713
E16.5	<i>Atf4</i> KO	Bulk RNA-Seq	Duncan	Germline KO	GSE206760	37998373
P0	<i>Celf1</i> cKO	Bulk RNA-Seq	Lachke	Pax6-Cre	GSE227293	37048143
P2	<i>Cryaa</i> Mt	Bulk RNA-Seq	Andley	<i>Cryaa</i> -R49C knock-in mutant	GSE98027	29338044
P4	<i>Tdrd7</i> KO	Bulk RNA-Seq	Tdrd7	Germline KO	GSE134384	32420594
P14	<i>Cryab</i> Mt	Bulk RNA-Seq	Andley	<i>Cryab</i> -R120G knock-in mutant	GSE98027	29338044
P30	<i>S100A4</i> KO	Bulk RNA-Seq	Rao	Germline cre deletion	GSE143909	33500475
P5, 20 weeks	<i>miR-26</i> Mt	Bulk RNA-Seq	Robinson	CRISPR/Cas9	GSE252611	38683565
8 weeks	<i>Fnl</i> cKO	Bulk RNA-Seq	Duncan	MLR10cre	GSE119878	32173580

Note: *E* = embryonic day; *P* = postnatal day; *KO* = knockout; *cKO* = conditional knockout; *Mt* = mutant.

2.2 Quality Control and Preprocessing

The quality of the raw sequencing reads was assessed using FastQC (v0.11.9) to evaluate base quality, biases, adapter contamination, or low-quality bases. Reads were then subjected to trimming and filtering using Cutadapt (v5.1) for adapter removal. A quality threshold of 20 was applied to retain high-confidence bases, and any remaining adapter sequences were eliminated to prevent mapping artifacts in downstream analyses. For samples with technical replicates, FastQ files were merged before trimming was performed.

2.3 Read Alignment

The mouse reference genome (GRCm39) and its corresponding annotation file

were downloaded from Ensembl. The genome was indexed using STAR (v2.7.10b) to enhance alignment efficiency. The trimmed reads were aligned to the reference genome using STAR with default parameters, ensuring high alignment accuracy and reproducibility. The resulting BAM files were sorted by coordinates to facilitate downstream analyses.

2.4 Gene Expression Quantification

To quantify gene expression, featureCounts (v2.0.3) was used to count aligned reads at both exon and gene levels. The annotation file was specified in the GTF format, and read assignment was performed based on gene identifiers. Since the datasets included both single-end and paired-end datasets, each BAM file was assessed using SAMtools to determine the appropriate parameters for featureCounts. Single-end and paired-end read counts were processed separately to maintain accuracy in quantification.

2.5 Differential Expression Analysis

Lowly expressed genes were filtered using `filterByExpr()` from edgeR, and normalization was applied using the Trimmed Mean of M-values (TMM) method via `calcNormFactors()`. Normalized data were then transformed using the voom function from the limma package and linear modeling was performed using `lmFit()` (with equation `model.matrix(~ 0 + group + batch)` where batch has the variables for laboratories that performed study), followed by empirical Bayes moderation with `eBayes()`. Differentially expressed genes (DEGs) were extracted using `topTreat()`, and significance was assessed based on $p\text{-value} < 0.05$ and a \log_2 fold change (\log_2FC) cutoff of $\geq |0.58|$, corresponding to a 1.5-fold change in expression.

2.6 Functional Enrichment Analysis

Significant DEGs were subjected to functional enrichment analysis using the enrichGO (clusterProfiler) package in R. Gene Ontology (GO) analysis was performed to identify enriched biological processes, cellular components and molecular functions. For some datasets, the online DAVID analysis tool was also used for GO analysis.

2.7 Data Visualization

To present the results effectively, various visualization techniques were employed. Volcano plots were generated using ggplot2 to illustrate the distribution of DEGs based on fold change and statistical significance. Additionally, hierarchical clustering and heatmap visualization were performed using pheatmap to depict expression patterns across samples. MA plots were also generated to visualize DEGs.

2.8 Statistical Analysis

The statistical significance of differential expression was evaluated using p-value or the Benjamini-Hochberg method to control for multiple testing. All statistical computations were performed in R, and significance thresholds were consistently applied across analyses.

Chapter 3

RESULTS

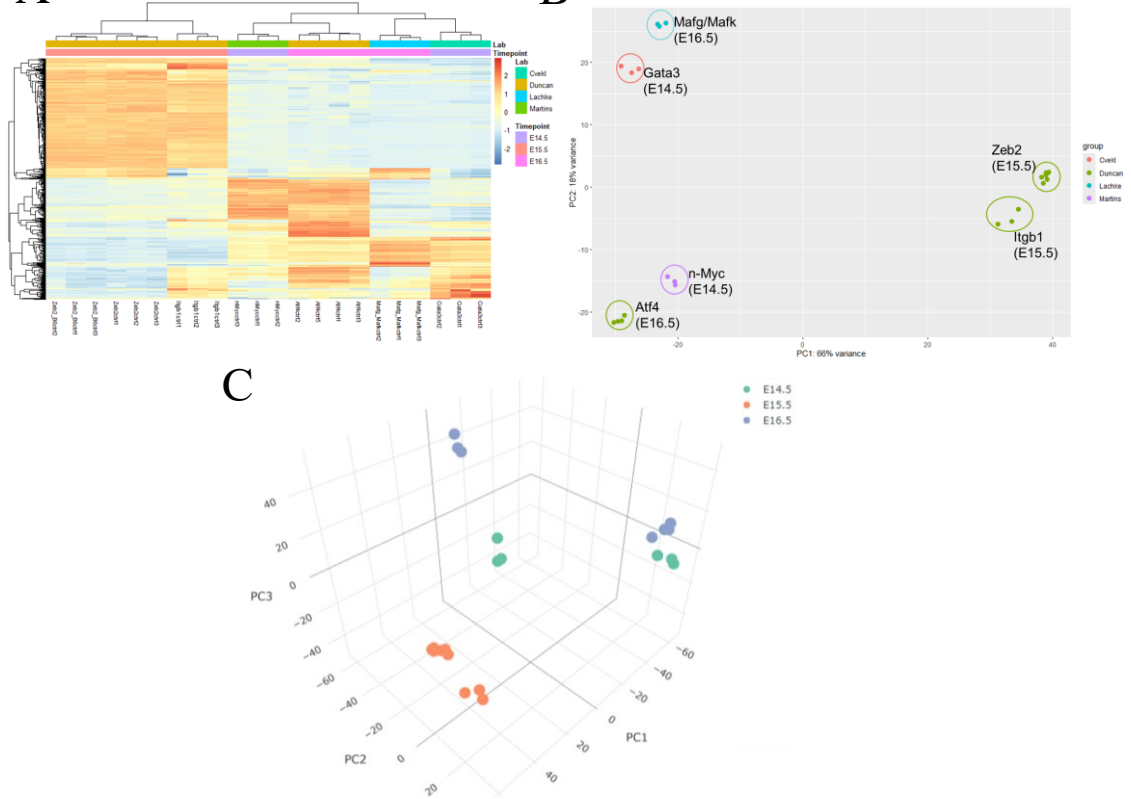
3.1 Clustering of embryonic control samples reveals developmental stage-specific patterns

Initial clustering analysis focused on assessing transcriptional variation among embryonic controls from the distinct studies was performed. The datasets comprised controls from E14.5 (N-myc and Gata3 controls), E15.5 (Zeb2 and Zeb2_B6 controls), E15.5 (Itgb1 controls) and E16.5 (Mafg/Mafk and Atf4 controls.) The control groups varied across individual studies and included different mouse strains and genetic backgrounds. For example, controls for the N-myc, Gata3, and Zeb2 studies were Cre-negative loxP/loxP mouse lenses, whereas Atf4 controls were wild-type, and Mafg/Mafk controls consisted of double heterozygous (Mafg^{+/-}/Mafk^{+/-}) lenses. Despite this inherent variability, the control samples clustered in a biologically coherent manner rather than lab of origin. A heatmap with hierarchical clustering of samples which was generated using the 500 topmost variable genes across all control samples shows separation of control samples that largely correspond to their embryonic stages (Figure 3.1A). Specifically, E15.5 control samples from both studies (Itgb1 and Zeb2) clustered closely together forming a branch, distinct from E14.5 and E16.5 controls.

To further evaluate clustering trends and potential batch effects, both two-dimensional and three-dimensional Principal Component Analysis (PCA) plots were generated (Figures 3B and 3C). The PCA plots also demonstrated that samples are primarily segregated by developmental timepoint along the first two principal

components. Together, these analyses validate stage-specific expression profiles in embryonic lens development and the observed clustering patterns support the biological

A istness of these datasets and provic **B** oundation for differential expression and



functional enrichment analyses.

Figure 3.1 Clustering of embryonic lens control samples based on transcriptomic profiles. (A) Heatmap of the top 500 most variable genes across embryonic lens control samples from multiple RNA-seq datasets, showing hierarchical clustering by developmental stage. (B) Principal Component Analysis (PCA) plot in two dimensions showing separation of control samples by developmental stage. (C) 3-Dimensional PCA plot illustrating enhanced separation of control samples. Each point represents one biological replicate; colors indicate developmental stage.

3.2 Differential expression analysis across embryonic lens cKO datasets

Differential expression analysis was performed by comparing all embryonic cKO samples collectively against all embryonic control samples. The test datasets included cKO samples from, E14.5 (N-myc and Gata3), E15.5 (Zeb2), E15.5 (Itgb1) and E16.5 (Atf4, Mafg/Mafk double and compound knockouts). Corresponding wild-type or Cre-ve control samples from each dataset together form the control group. The control sample in the Mafg/Mafk datasets are Mafg^{+/-}/Mafk^{+/-}. Given the diversity of sequencing platforms, sample sizes, and developmental stages represented across the datasets, an unadjusted p-value threshold of 0.05 was applied here. Adjusted p-values (e.g., Benjamini-Hochberg) were found to be overly conservative in this multi-study context and could potentially exclude biologically meaningful signals.

Table 3.1 Differentially expressed genes between embryonic KO and control lens samples using unadjusted p-value < 0.05.

Down-regulated genes	131
Not significant	14517
Up-regulated genes	154

Table 3.2 Differentially expressed genes using adjusted p-value < 0.05.

Down-regulated genes	21
Not significant	14771
Up-regulated genes	10

Statistical significance was determined using raw p-values < 0.05 alongside a log₂ fold change (log₂FC) cutoff of $\geq |0.58|$, corresponding to a 1.5-fold change in expression. Using the p-value threshold (Table 3.1), 154 genes were found to be upregulated and 131 were downregulated across all embryonic cKO datasets, while 14,517 genes were not significantly changed. In contrast, the Benjamini-Hochberg-adjusted p-value cutoff < 0.05 (Table 3.2) yielded only 31 DEGs which comprised 10 upregulated and 21 downregulated genes, with 14,771 genes called not significant.

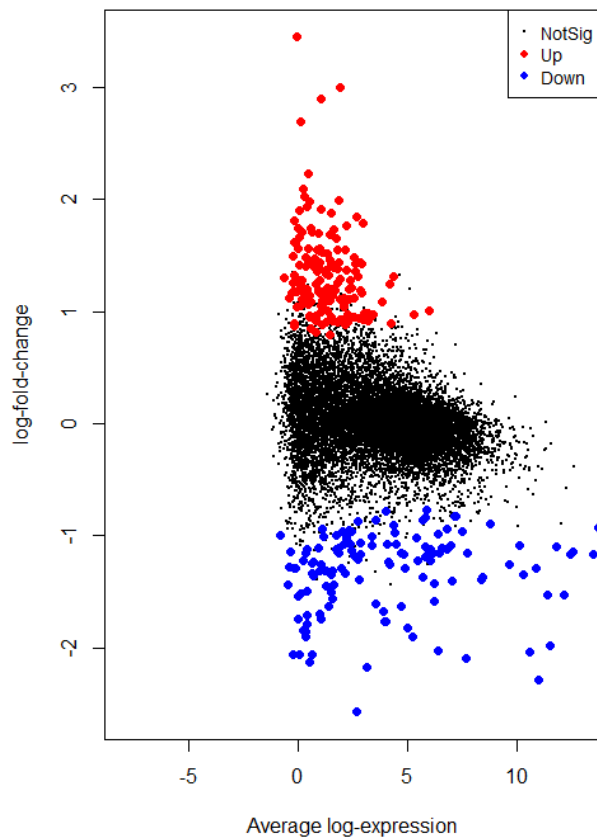


Figure 3.2 Differential expression analysis of embryonic lens KO samples versus controls. MA plot showing average log expression (x-axis) versus log₂ fold change (y-axis) across all embryonic samples. Red points indicate significantly upregulated genes; blue points indicate downregulated genes ($\text{Log}_2\text{FC} \geq |0.58|$, p-value < 0.05).

The MA plot showing average log expression (mean of normalized counts) versus log fold change demonstrates the distribution of differentially expressed genes (DEGs) (Figure 3.2). The identified DEGs provide a basis for downstream functional analyses aimed at identifying conserved regulatory pathways disrupted during embryonic lens development. Additionally, the volcano plot reveals a distinct subset of genes showed strong upregulation or downregulation in the embryonic cKO group compared to controls (Figure 3.3).

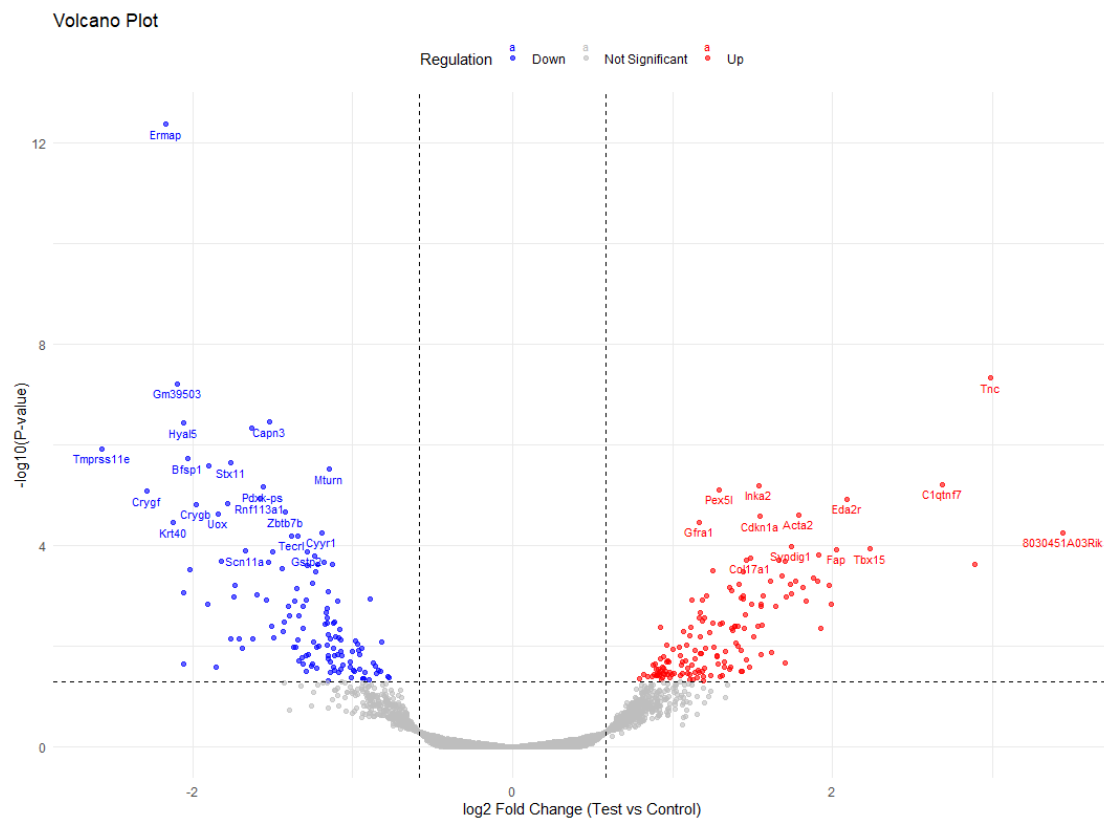


Figure 3.3 Volcano plot of differentially expressed genes in embryonic lens KO samples. Log₂ fold change versus $-\log_{10}$ p-value. Red and blue dots represent significantly upregulated and downregulated genes, respectively ($\log_2\text{FC} \geq |0.58|$, $p\text{-value} < 0.05$). Labeled genes represent top 40 DEGs.

3.3 Lens expression profiles of top differentially expressed genes

To investigate the relevance of the most significantly misregulated genes in embryonic lens cKOs, the top 20 upregulated genes (Table 1) and top 20 downregulated genes (Table 2) (ranked by fold change and p-value) were analyzed for their spatiotemporal expression patterns in the lens using the iSyTE (integrated Systems Tool for Eye gene discovery) database. Many strongly downregulated genes have well-established roles in lens development and transparency. These include *Crygf*, *Crygn* and *Crygb*, which encode γ -crystallins essential for lens fiber cell structure and refractive properties. *Bfsp1* encodes a lens-specific intermediate filament protein which is critical for maintaining fiber cell integrity. *Dnase2b* encodes a nuclease required for denucleation during terminal lens fiber differentiation. The full list of top upregulated and downregulated genes is provided in the Appendix.

Each list of the top 20 genes was queried separately in iSyTE. The results revealed a striking difference between upregulated and downregulated gene sets with respect to their normal expression patterns in the lens. Almost all upregulated genes exhibited low expression across all developmental stages (Figure 3.4A) and were generally not enriched in the lens relative to whole embryonic body tissues (Figure 3.4B). These genes possibly represent non-lens specific transcriptional programs that become aberrantly activated upon gene knockout, possibly due to loss of lens-specific repression. Alternatively, they could be a consequence of stress-response or inflammatory pathways. These may also reflect compensatory or non-specific responses to genetic perturbation. The top 20 downregulated gene set showed a markedly different pattern instead. Most of these genes are robustly expressed in the lens during normal embryonic development (Figure 3.5A) and exhibit high lens-enrichment scores in iSyTE during embryonic lens development (Figure 3.5B). Many of these genes are

known to play critical roles in lens structure and function, including cytoskeletal organization (*Bfsp1*), and crystallin expression (*Crygf*, *Crygb*). The consistent downregulation across the cKO samples suggests the disruption of genes essential for proper lens development.

Table 3.3 Top 20 upregulated genes in embryonic lens KO samples

	Symbol	Gene description	Entrez	Fold Change	P.Value
1	8030451A03Rik	RIKEN cDNA 8030451A03 gene	100504061	10.88	5.50E-05
2	Tnc	tenascin C	21923	7.95	4.74E-08
3	Mt1	metallothionein 1	17748	7.42	0.00023547
4	C1qtnf7	C1q and tumor necrosis factor related protein 7	109323	6.43	6.06E-06
5	Tbx15	T-box 15	21384	4.70	0.00011521
6	Eda2r	ectodysplasin A2 receptor	245527	4.26	1.20E-05
7	Fap	fibroblast activation protein	14089	4.07	0.00011845
8	Dcn	decorin	13179	3.98	0.00146312
9	Fbln5	fibulin 5	23876	3.95	0.00062532
10	Adamts2	ADAM metalloproteinase with thrombospondin type 1 motif 2	216725	3.81	0.00441745
11	Aass	aminoadipate-semialdehyde synthase	30956	3.77	0.00015369
12	Sstr1	somatostatin receptor 1	20605	3.75	0.00051384
13	Lox	lysyl oxidase	16948	3.69	0.00044507
14	Dlk1	delta like non-canonical Notch ligand 1	13386	3.58	0.0012422
15	Pdlim3	PDZ and LIM domain 3	53318	3.52	0.00067714
16	Acta2	actin alpha 2, smooth muscle, aorta	11475	3.45	2.46E-05
17	Radil	Ras association and DIL domains	231858	3.41	0.00050864
18	Svep1	sushi, von Willebrand factor type A, EGF and pentraxin domain containing 1	64817	3.36	0.00089322
19	Syndig1	synapse differentiation inducing 1	433485	3.35	0.00010272
20	Alx4	aristaless-like homeobox 4	11695	3.33	0.00059559



Figure 3.4. iSyTE expression and enriched expression profile of the top 20 upregulated genes in embryonic lens KO samples. Heatmap showing expression (A) and enriched expression (B) of the top upregulated DEGs in mouse lens stages. Note: Not all 20 genes were found in the iSyTE database; the heatmap includes only those with available data

Table 3.4. Top 20 downregulated genes in embryonic lens KO samples

	Symbol	Gene description	Entrez	Fold Change	P.Value
1	Tmprss11e	transmembrane protease, serine 11e	243084	-5.94	1.20536633423036e-06
2	Crygf	crystallin, gamma F	12969	-4.89	8.34893953977551e-06
3	Ermap	erythroblast membrane-associated protein	27028	-4.51	4.29709888927845e-13
4	Krt40	keratin 40	406221	-4.36	3.52514421942051e-05
5	Gm39503	predicted gene, 39503	105243672	-4.28	6.08893662664666e-08
6	Gm52334	predicted gene, 52334	115488904	-4.17	0.000856911
7	Hyal5	hyaluronoglucosaminidase 5	74468	-4.17	3.71128131045758e-07
8	1700071M16Rik	RIKEN cDNA 1700071M16 gene	73504	-4.16	0.022250562
9	Bfsp1	beaded filament structural protein 1, in lens-CP94	12075	-4.09	1.88773615272597e-06
10	Bcl	brain cytoplasmic RNA 1	100568459	-4.06	0.000304623
11	Crygb	crystallin, gamma B	12965	-3.94	1.50750415995132e-05
12	Tmem252	transmembrane protein 252	226040	-3.74	0.001477432
13	Myo7b	myosin VIIB	17922	-3.73	2.5672197331593e-06
14	Gm32014	predicted gene, 32014	102634431	-3.62	0.025344486
15	Uox	urate oxidase	22262	-3.59	2.35822627822451e-05
16	Dnase2b	deoxyribonuclease II beta	56629	-3.53	0.000202066
17	Gm36264	predicted gene, 36264	102640119	-3.44	1.46959638647723e-05
18	Stx11	syntaxin 11	74732	-3.39	2.31046953800952e-06
19	E130119H09Rik	RIKEN cDNA E130119H09 gene	78550	-3.39	0.007009556
20	Gm52729	predicted gene, 52729	115489984	-3.35	0.001023698

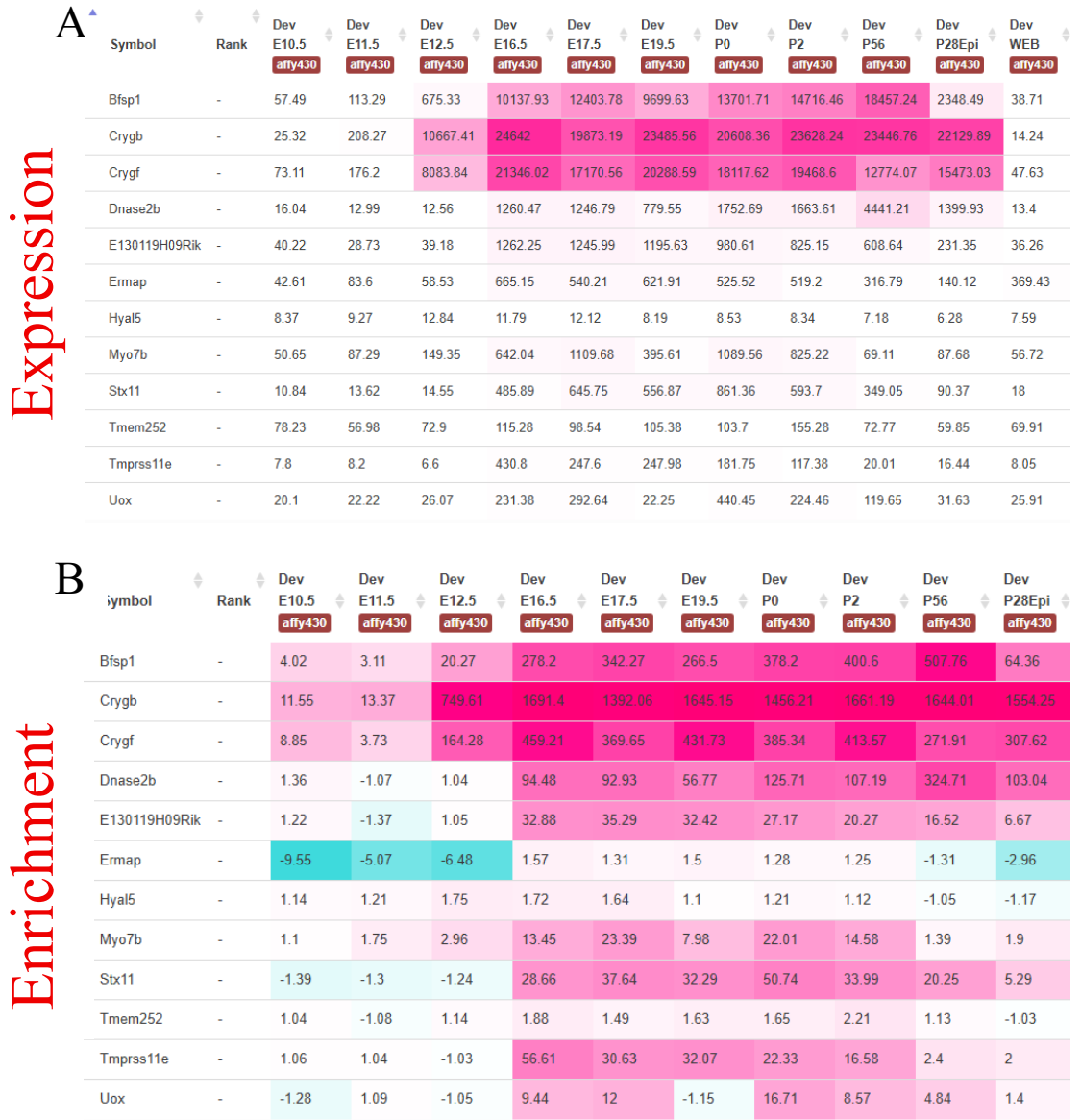


Figure 3.5. iSyTE expression profile of the top 20 downregulated genes in embryonic lens KO samples. Heatmap of downregulated DEGs showing high expression (A) and strong lens enrichment (B) during embryonic development, consistent with roles in lens structure and function. Note: Only genes with available expression data in iSyTE are shown

3.4 Gene ontology enrichment reveals functional disruption of lens-specific processes in embryonic KO lenses

To gain functional insights into the biological consequences of gene misregulation in the embryonic cKO lens samples, Gene Ontology (GO) enrichment analysis was performed using the `enrichGO` function in R. DEGs from the combined embryonic cKO versus control comparison were analyzed across three major GO domains: Biological Process (BP), Cellular Component (CC), and Molecular Function (MF). Enrichment results were visualized as dot plots, and separate analyses were also conducted for upregulated and downregulated DEGs. The Cellular Component enrichment analysis (Figure 3.6A) highlighted significant terms related to structural and extracellular organization such as “extracellular matrix”, “external encapsulating structure”, “intermediate filament cytoskeleton”, and “sodium channel complex”, suggesting that the misregulated genes encode structural or membrane-associated components important for lens architecture and signaling. The Biological Process analysis of all DEGs (Figure 3.6B) revealed enrichment in lens-specific and developmental functions. Notably enriched terms included “sensory perception”, “eye development”, “camera-type eye development”, and more specifically, “lens development in camera-type eye”. In addition, processes like “intermediate filament cytoskeleton organization” were also significantly overrepresented, reflecting disruption of fiber cell differentiation and cytoskeletal remodeling. In the Molecular Function category (Figure 3.6C), enriched terms include “structural molecule activity”, “integrin binding”, “transmembrane transporter activity”, and “signaling receptor regulator activity”. Importantly, “structural constituent of eye lens” was also among the top enriched terms.

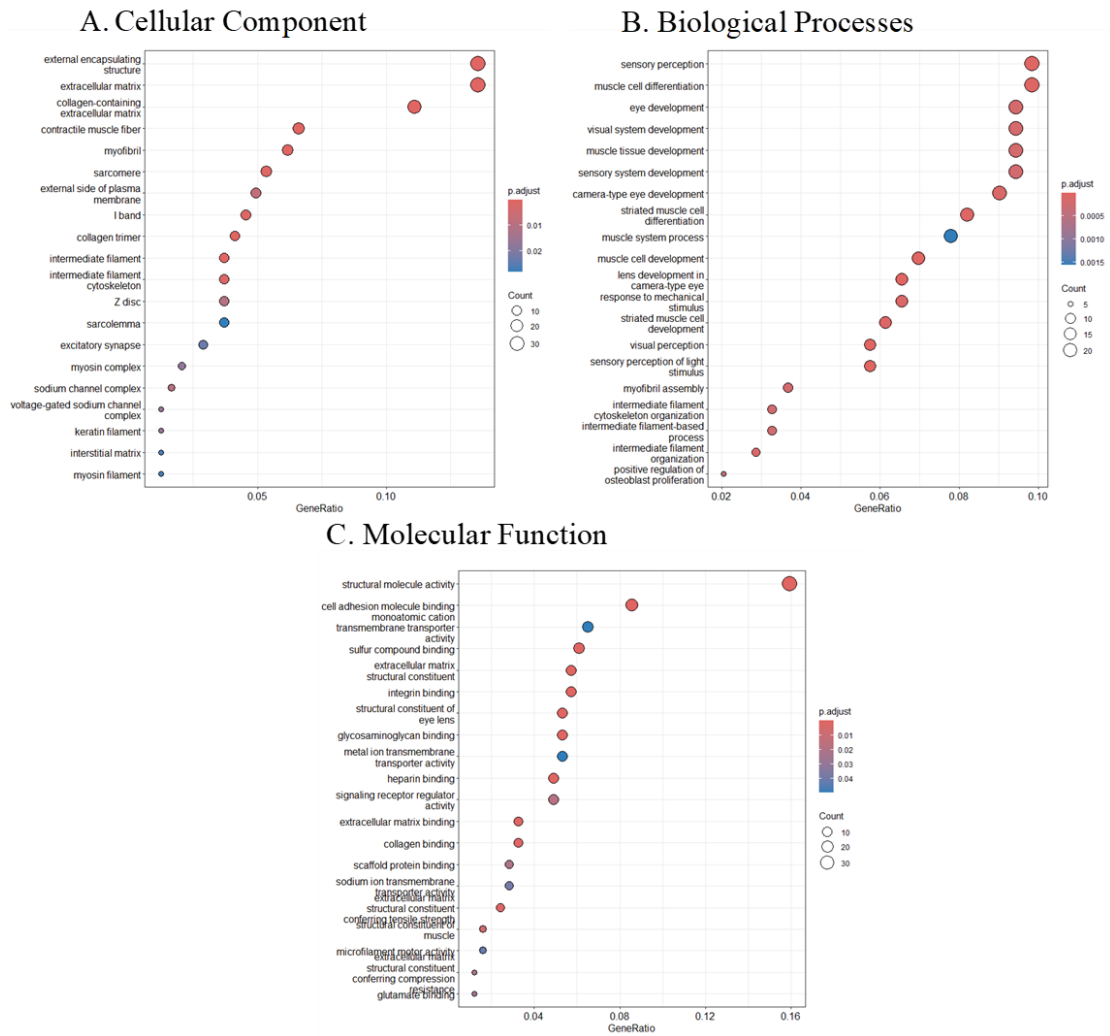
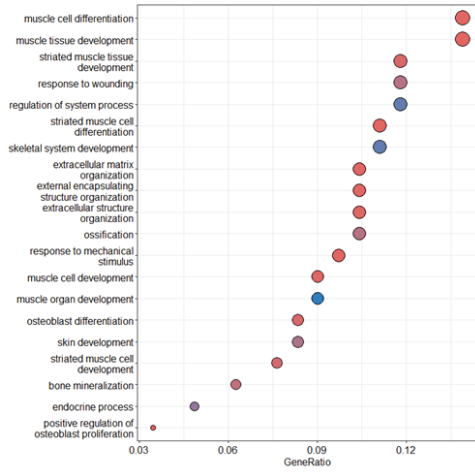


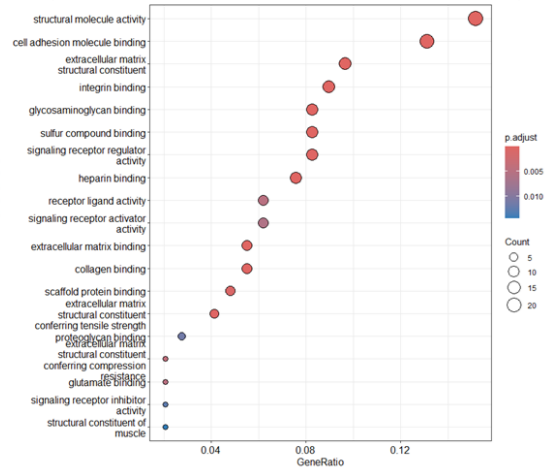
Figure 3.6 Gene Ontology enrichment dot plots for all DEGs in embryonic lens cKO samples (A) Cellular Component (CC) terms enriched in DEGs, (B) Biological Process (BP) terms enriched in DEGs, (C) Molecular Function (MF) terms enriched in DEGs

Separate GO analyses of upregulated and downregulated genes (Figures 3.7A–D) also revealed clear functional asymmetry. Upregulated genes were enriched in non-lens-biological processes, many of which are not typically active in the lens including “muscle cell differentiation”, “response to wounding”, “regulation of system process”, “skin development”, and “osteoblast differentiation”, possibly reflecting stress or compensatory signaling in the knockout lenses. In terms of molecular function, upregulated genes were enriched in categories such as “signaling receptor regulator activity”, “extracellular matrix structural constituent”, and “heparin binding”. Conversely, downregulated genes were predominantly enriched in lens-specific structural and developmental processes, highlighting the loss of key regulators and effectors of lens formation. BP terms includes “lens development in camera-type eye”, “lens fiber cell differentiation”, “eye development”, “sensory perception”, “visual perception”, and “visual system development”. These enriched categories suggest that proper lens development is consistently hampered across all the knockout lens samples. Additionally, corresponding MF enrichment for downregulated genes include significant terms such as “structural molecule activity” and “structural constituent of eye lens”.

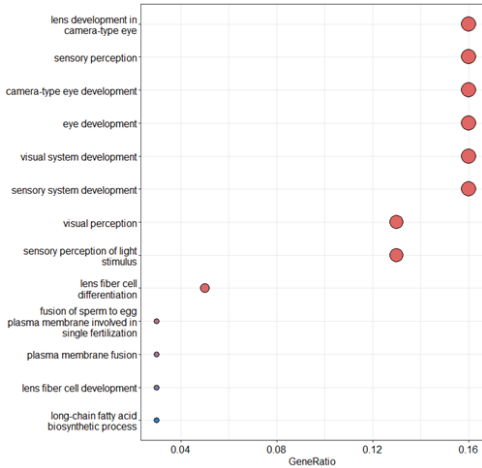
A. Biological Processes (UP genes)



B. Molecular Function (UP genes)



C. Biological Processes (Down genes)



D. Molecular Function (Down genes)

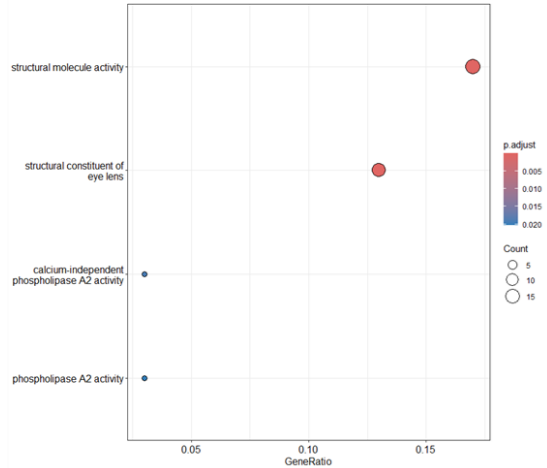


Figure 3.7 GO enrichment dot plots for upregulated and down regulated DEGs in embryonic KO lenses. (A) BP terms for upregulated genes. (B) MF terms for upregulated genes. (C) BP terms for downregulated genes (D) MF terms for downregulated genes

3.5 GO enrichment analysis of 31 high-confidence DEGs highlights lens-specific functions

To focus on the most statistically robust transcriptional changes, GO enrichment was performed on the 31 DEGs that passed a stringent false discovery rate (FDR-adjusted p-value < 0.05 and log₂ fold change ≥ |0.58|) using the online DAVID analysis. Although more limited in number, this high-confidence gene set revealed a strong and focused enrichment in lens-related biological functions and cellular components (Figure 3.8). In the Biological Process (BP) category, the genes were significantly enriched for terms directly related to ocular development, including “lens development in camera-type eye” and “lens fiber cell differentiation”. These findings show that despite cross-study heterogeneity, certain lens developmental programs are consistently disrupted across embryonic lens cKOs. Top enriched terms in Cellular Component include “plasma membrane” and “intermediate filament”, suggesting that disruptions to these localizations may underlie or drive the disease/defective phenotypes in embryonic lens cKOs. In the Molecular Function (MF) category, “structural constituent of eye lens” was also significantly enriched.

Biological Process						
Category	Term	RT	Genes	Count	%	P-Value
GOTERM_BP_DIRECT	lens development in camera-type eye	RT		3	9.7	7.5E-4
GOTERM_BP_DIRECT	eye development	RT		3	9.7	1.1E-3
GOTERM_BP_DIRECT	visual perception	RT		3	9.7	7.0E-3
GOTERM_BP_DIRECT	lens fiber cell development	RT		2	6.5	7.5E-3
GOTERM_BP_DIRECT	programmed cell death	RT		2	6.5	3.0E-2
GOTERM_BP_DIRECT	regulation of G1/S transition of mitotic cell cycle	RT		2	6.5	5.3E-2
GOTERM_BP_DIRECT	intermediate filament organization	RT		2	6.5	6.0E-2
GOTERM_BP_DIRECT	positive regulation of gene expression	RT		3	9.7	8.6E-2
GOTERM_BP_DIRECT	positive regulation of JNK cascade	RT		2	6.5	9.5E-2
Cellular Component						
Category	Term	RT	Genes	Count	%	P-Value
GOTERM_CC_DIRECT	plasma membrane	RT		10	32.3	6.5E-2
GOTERM_CC_DIRECT	brush border	RT		2	6.5	7.5E-2
GOTERM_CC_DIRECT	external side of plasma membrane	RT		3	9.7	8.3E-2
GOTERM_CC_DIRECT	intermediate filament	RT		2	6.5	8.5E-2
Molecular Function						
Category	Term	RT	Genes	Count	%	P-Value
GOTERM_MF_DIRECT	structural constituent of eye lens	RT		4	12.9	1.9E-6
GOTERM_MF_DIRECT	protein kinase binding	RT		3	9.7	9.8E-2

Figure 3.8 Gene Ontology analysis of the 31 DEGs identified using FDR cutoff (adjusted p-value < 0.05) across embryonic lens cKO datasets. GO analysis was performed using DAVID, and enriched terms are shown across the three categories.

3.6 Early postnatal lens control samples cluster according to developmental stage and similar gene expression profiles

To evaluate transcriptional relationships among early postnatal control lens samples (P0, P2, P4 and P5), I performed unsupervised clustering using both hierarchical heatmap analysis and 3-D PCA based on normalized gene expression data. The heatmap of the top 500 most variable genes (Figure 3.9A) revealed partial stage-dependent clustering patterns among the samples. P2 (Cryaa) and P14 (Cryab) controls

formed a distinct subcluster and interestingly both are derived from the C57BL/6J mouse background. In contrast, the remaining samples including P0 (Celf1, mixed C57BL/6J/FVB/N), P4 (Tdrd7, heterozygous mixed background), and P5 (mir-26, FVB/N) clustered separately, likely reflecting both developmental and strain-specific transcriptomic differences. The 3-D PCA plot (Figure 3.9B) however provided clearer separation along principal component 1 (PC1) in a manner that reflected developmental progression. Notably, P0 (Celf1) and P2 (Cryaa) clustered closely, while P4 (Tdrd7) and P5 (mir-26) cluster in the middle between P14 and P0/P2 suggesting early postnatal transcriptional similarity. P4 (Tdrd7) and P5 (mir-26) occupied an intermediate position between the early (P0/P2) and later (P14) timepoints. This PCA-based clustering supports their inclusion in this integrated meta-analysis despite differences in strain background.

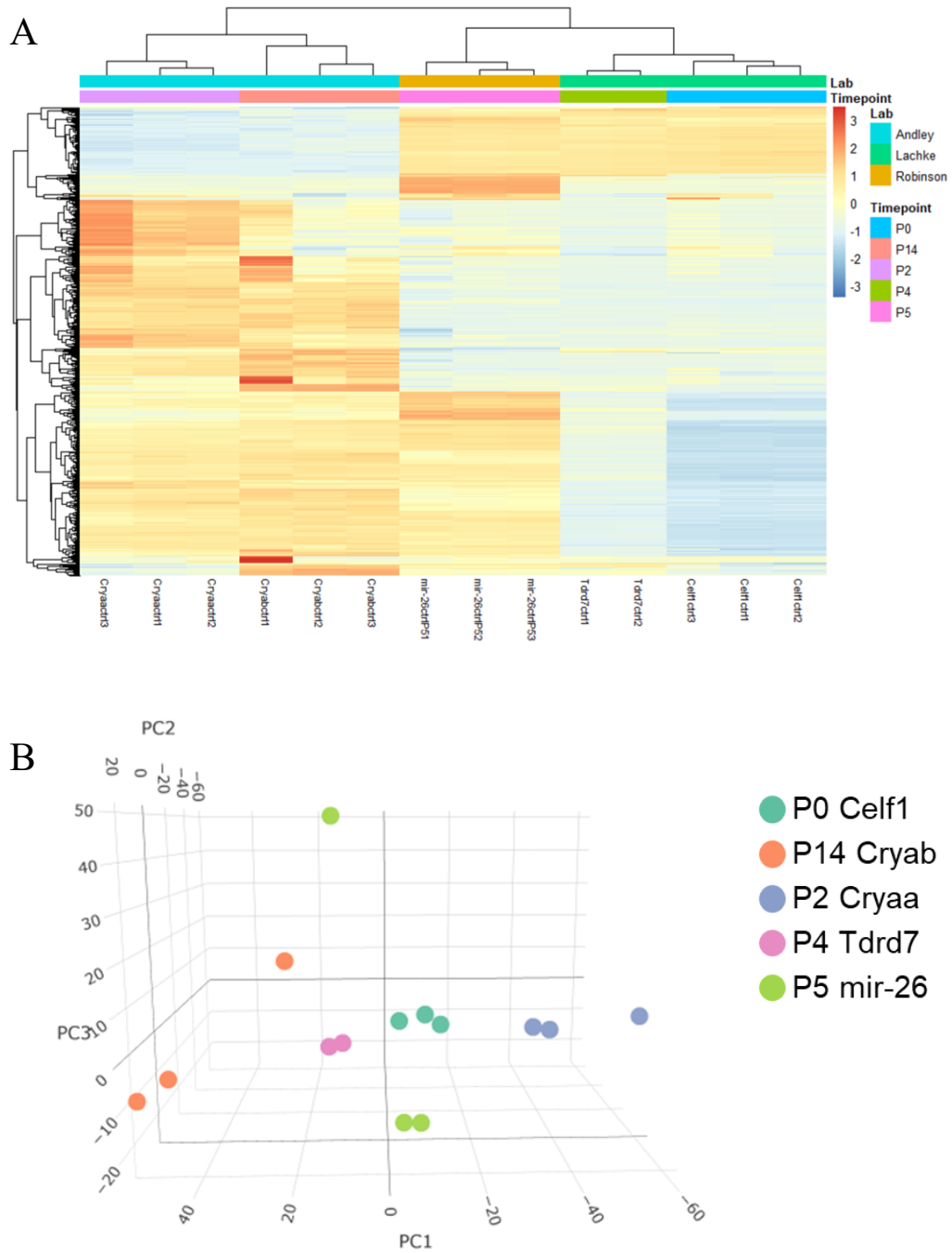


Figure 3.9 Clustering analysis of early postnatal lens control samples.(A) Heatmap of the top 500 most variable genes across early postnatal control samples.(B) 3-D PCA plot showing spatial separation of control samples.

3.7 Differential expression analysis reveals limited but targeted misregulation across early postnatal cKOs

To identify genes significantly altered in early postnatal lens cKO samples, I performed differential expression analysis comparing all cKO samples (Cryaa P2, Cryab P14, mir-26 P5, Tdrd7 P4, Celf1 P0) to their controls. I applied a \log_2 fold change (Log2FC) threshold of $\geq |0.58|$ (equivalent to a 1.5-fold change) and a p-value cutoff of 0.05. This analysis yielded a total of 36 differentially expressed genes, including 23 downregulated and 13 upregulated genes (Table 3.5). The remaining 12,700 genes did not meet the significance threshold. The volcano plot (Figure 3.10) visualizes the overall distribution of gene expression changes, with significantly upregulated and downregulated genes clearly labeled.

Table 3.5 Differentially expressed genes between early postnatal lens cKO and controls using unadjusted p-value < 0.05

Down-regulated genes	23
Not significant	12700
Up-regulated genes	13

I utilized iSyTE to analyze the expression and enrichment patterns of the upregulated and downregulated gene sets in normal WT. The full lists of 13 upregulated (Table 3.6) and 23 downregulated genes (Table 3.7) were submitted separately to iSyTE, and their spatiotemporal expression across mouse lens developmental stages was examined. The upregulated genes displayed generally low expression in WT lens across development, with little to no enrichment in lens tissue relative to whole embryonic body controls (Figure 3.11). This pattern suggests that these genes are not lens-specific and may reflect indirect or stress-related transcriptional changes in the cKO models. Notably, several of these genes including *Prph2*, *Pdc*, *Pde6b*, and *Sag* are well-

established retinal-specific genes, suggesting that retinal programs can be activated in the lens under conditions of gene perturbation. Conversely, the downregulated genes demonstrated good expression in the lens and high enrichment scores in iSyTE, particularly during late embryonic (E16.5–E19.5) and early postnatal (P0–P2) stages (Figure 3.12). Many of these genes showed a marked increase in expression beginning in late embryogenesis and early postnatal stages.

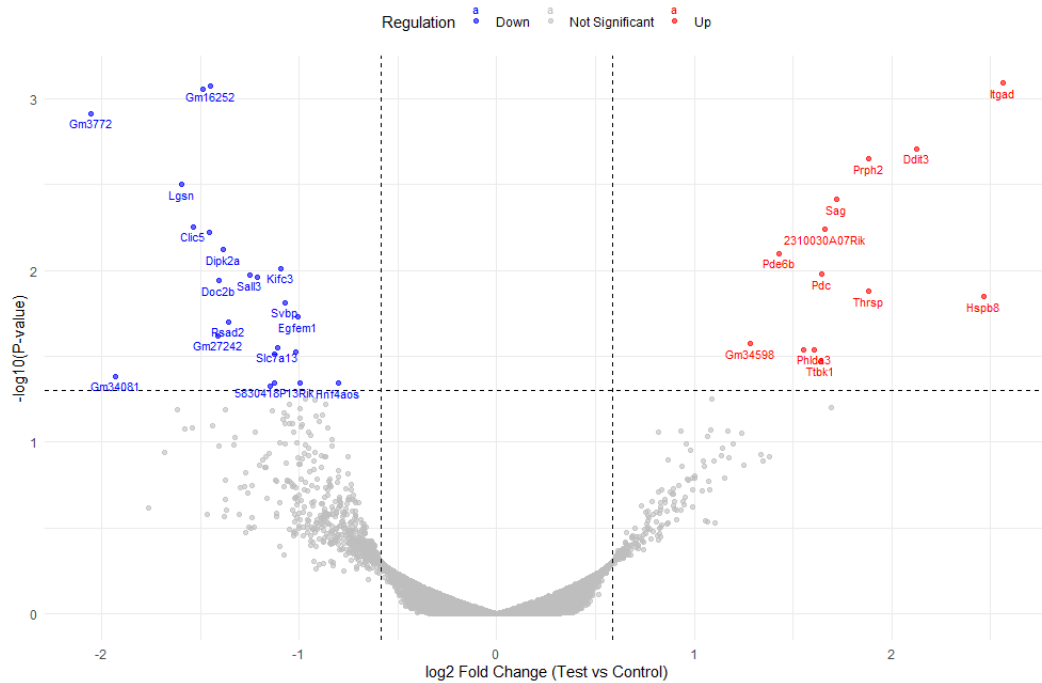


Figure 3.10 Volcano plot of differentially expressed genes in early postnatal lens cKO samples. All 36 DEGs are labelled

Table 3.6 List of 13 upregulated DEGs in early postnatal lens KOs

Symbol	Gene description	Entrez	Fold Change	P.Value
Itgad	integrin, alpha D	381924	5.92	0.00081
Hspb8	heat shock protein 8	80888	5.52	0.014232
Ddit3	DNA-damage inducible transcript 3	13198	4.37	0.001962
Prph2	peripherin 2	19133	3.69	0.002234
Thrsp	thyroid hormone responsive	21835	3.69	0.013279
Sag	S-antigen, retina and pineal gland (arrestin)	20215	3.29	0.003857
2310030A07Rik	RIKEN cDNA 2310030A07 gene	75584	3.17	0.005767
Pdc	phosducin	20028	3.13	0.010567
Ttbk1	tau tubulin kinase 1	106763	3.11	0.033811
Phlda3	pleckstrin homology like domain, family A, member 3	27280	3.05	0.029
Trp53inp1	transformation related protein 53 inducible nuclear protein 1	60599	2.93	0.029149
Pde6b	phosphodiesterase 6B, cGMP, rod receptor, beta polypeptide	18587	2.69	0.007969
Gm34598	predicted gene, 34598	102637902	2.43	0.026696

Table 3.7 List of 23 downregulated DEGs in early postnatal lens KOs

Symbol	Gene description	Entrez	Fold Change	P.Value
Gm3772	predicted gene 3772	100042291	-4.16	0.001217
Gm34081	predicted gene, 34081	102637209	-3.81	0.041471
Lgsn	lengsin, lens protein with glutamine synthetase domain	266744	-3.03	0.003165
Clic5	chloride intracellular channel 5	224796	-2.90	0.005556
Slc2a9	solute carrier family 2 (facilitated glucose transporter), member 9	117591	-2.80	0.000887
Gm31036	predicted gene, 31036	102633132	-2.74	0.005998
Gm16252	predicted gene 16252	102643244	-2.74	0.000848
Gm27242	predicted gene 27242	102632843	-2.67	0.024022
Doc2b	double C2, beta	13447	-2.65	0.011495
Dipk2a	divergent protein kinase domain 2A	68861	-2.62	0.007594
Rsad2	radical S-adenosyl methionine domain containing 2	58185	-2.56	0.019889
Sall3	spalt like transcription factor 3	20689	-2.38	0.010656
E130119H09Rik	RIKEN cDNA E130119H09 gene	78550	-2.32	0.010902
Ppm1e	protein phosphatase 1E (PP2C domain containing)	320472	-2.21	0.047104
Rnf180	ring finger protein 180	71816	-2.19	0.03089
5830418P13Rik	RIKEN cDNA 5830418P13 gene	100529079	-2.18	0.044957
Slc7a13	solute carrier family 7, (cationic amino acid transporter, y+ system) member 13	74087	-2.16	0.028128
Kifc3	kinesin family member C3	16582	-2.14	0.009768
Svbp	small vasohibin binding protein	69216	-2.10	0.015369
Tcp11	t-complex protein 11	21463	-2.02	0.029879
Egfem1	EGF-like and EMI domain containing 1	75740	-2.01	0.018688
Sned1	sushi, nidogen and EGF-like domains 1	208777	-2.00	0.045542
Hnf4aos	hepatic nuclear factor 4 alpha, opposite strand	68314	-1.74	0.045441

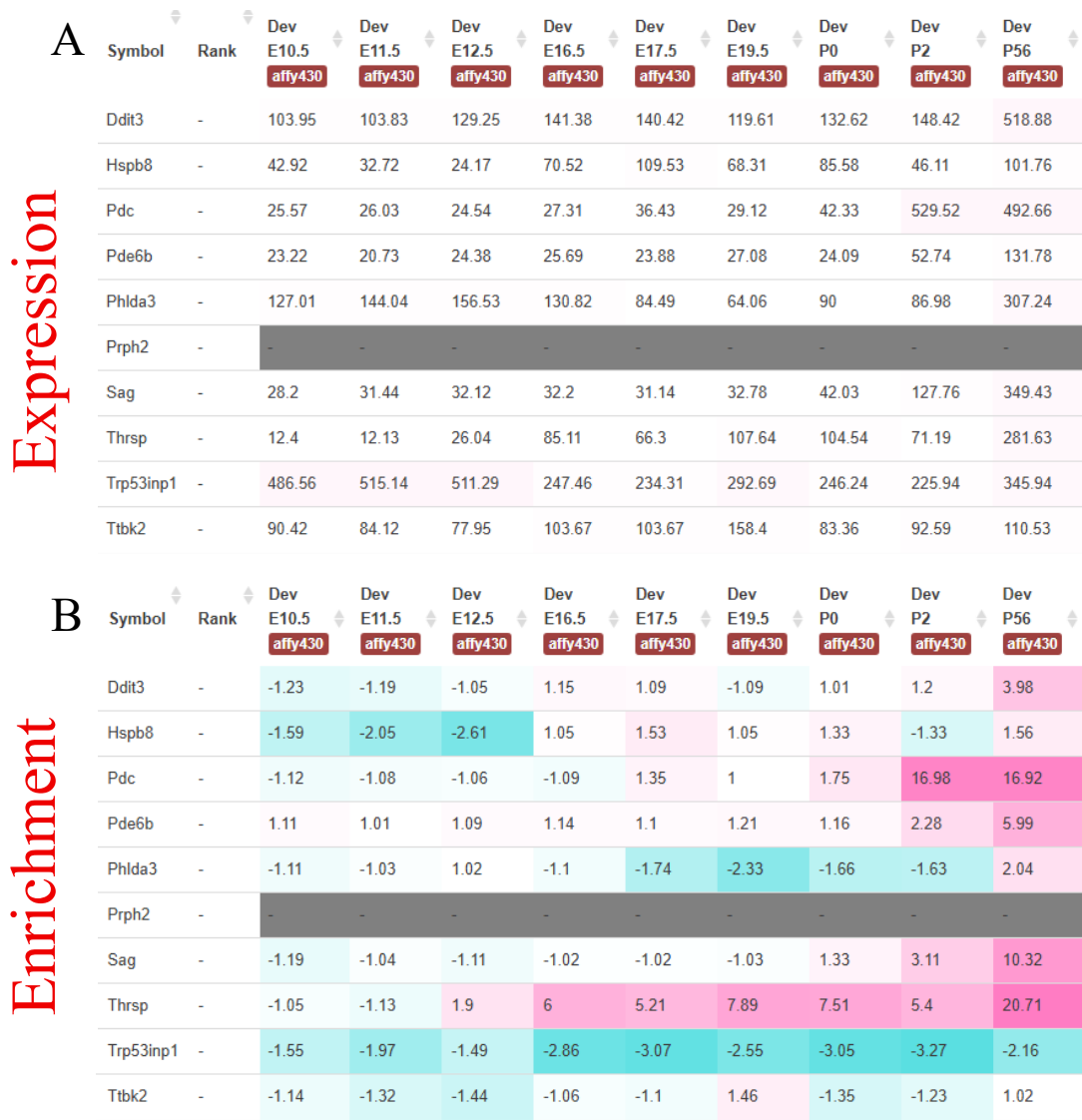


Figure 3.11 iSyTE analysis of upregulated DEGs from early postnatal KO lenses (A) Expression and (B) lens enrichment patterns for upregulated DEGs across mouse lens developmental stages.

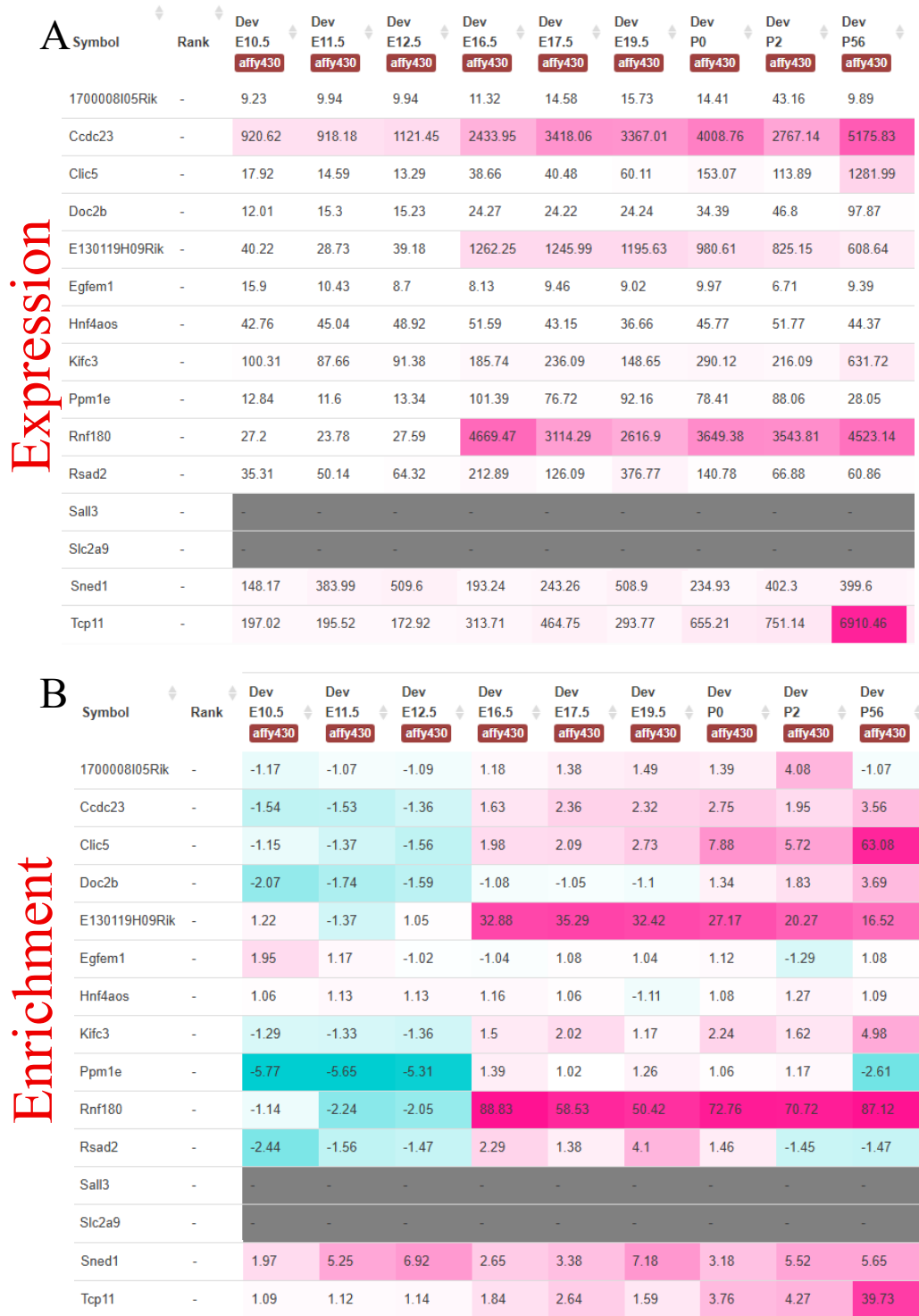


Figure 3.12 iSyTE analysis of downregulated DEGs from early postnatal KO lenses (A) Expression and (B) lens enrichment patterns for downregulated DEGs across mouse lens developmental stages.

3.8 GO analysis of upregulated genes reveals abnormal retinal gene expression in early postnatal KO lens

To further investigate the functional significance of the upregulated genes in early postnatal cKO lenses, I performed Gene Ontology (GO) analysis using the online DAVID functional annotation tool. This analysis revealed enriched Biological Process (BP) terms including “visual perception,” “retina development in camera-type eye,” and “positive regulation of apoptotic process” (Table 3.8). Importantly, unlike in the embryonic datasets where visual system-related terms were enriched due to the downregulation of authentic lens-expressed genes, the enrichment of “visual perception” in this context is driven by the upregulation of known retinal genes such as *Prph2*, *Pdc*, *Pde6b*, and *Sag*. These genes are typically restricted to photoreceptor cells in the retina and are not expressed in the lens under physiological conditions. This abnormal retinal gene expression was further supported by Cellular Component (CC) enrichment results with terms including “photoreceptor outer segment” and “photoreceptor inner segment”, which are regions specific to retinal photoreceptor cells (Table 3.9). These findings strongly suggest that disruption of normal postnatal transcriptional regulation in the lens allows inappropriate expression of non-lens, retina-restricted genes.

3.9 Functional categorization of downregulated genes in early postnatal lens KOs

To explore the biological roles of the 23 downregulated genes identified in the early postnatal lens knockouts, I first conducted Gene Ontology (GO) enrichment analysis using both enrichGO and DAVID. However, neither tool returned statistically significant enrichment results. Despite this limitation, I manually curated and functionally grouped the downregulated genes based on known biological roles and

published literature. This categorization revealed that some of these genes are functionally associated with ion and solute transport (*Slc2a9*, *Slc7a13*, *Clic5*), and cytoskeletal organization (*Dipk2a*, *Kifc3*), . These biological themes are critical for maintaining lens homeostasis. These findings suggest that, despite the small DEG size, it includes biologically meaningful genes whose collective downregulation may contribute to the disruption of lens maintenance in cKO conditions.

Table 3.8 Gene Ontology (BP) analysis of upregulated genes in early postnatal KO lenses

Category	Term	Genes	PValue
GOTERM BP DIRECT	GO:0007601~visual perception	Prph2, Pde6b, Pdc	0.001351
GOTERM BP DIRECT	GO:0043065~positive regulation of apoptotic process	Ddit3, Phlda3, Trp53inp1	0.009132
GOTERM BP DIRECT	GO:0051898~negative regulation of phosphatidylinositol 3-kinase/protein kinase B signal transduction	Ddit3, Phlda3	0.027062
GOTERM BP DIRECT	GO:0060041~retina development in camera-type eye	Prph2, Pde6b	0.039628
GOTERM BP DIRECT	GO:0007165~signal transduction	Sag, Pde6b, Ttbk1	0.044198

Table 3.9 Gene Ontology (CC) analysis of upregulated genes in early postnatal KO lenses

Category	Term	Genes	PValue
GOTERM CC DIRECT	GO:0001750~photoreceptor outer segment	Prph2, Sag, Pde6b, Pdc	3.17E-06
GOTERM CC DIRECT	GO:0001917~photoreceptor inner segment	Prph2, Sag, Pdc	0.000359
GOTERM CC DIRECT	GO:0005634~nucleus	Hspb8, Ddit3, Thrsp, Ttbk1, Pdc, Trp53inp1	0.052813
GOTERM CC DIRECT	GO:0005829~cytosol	Hspb8, Thrsp, Ttbk1, Pdc, Trp53inp1	0.064917

3.10 Clustering of Adult Control Lens Samples

The 3-D PCA plot (Figure 3.13) of normalized gene expression data from adult control lens samples (P30 S100A4, 8-weeks Fn1, and 20-week mir-26) revealed distinct clustering patterns based on age. The main separation occurred along principal components 1 and 2 (PC1 and PC2). Biological replicates within each group clustered closely together and were clearly separated from other groups.

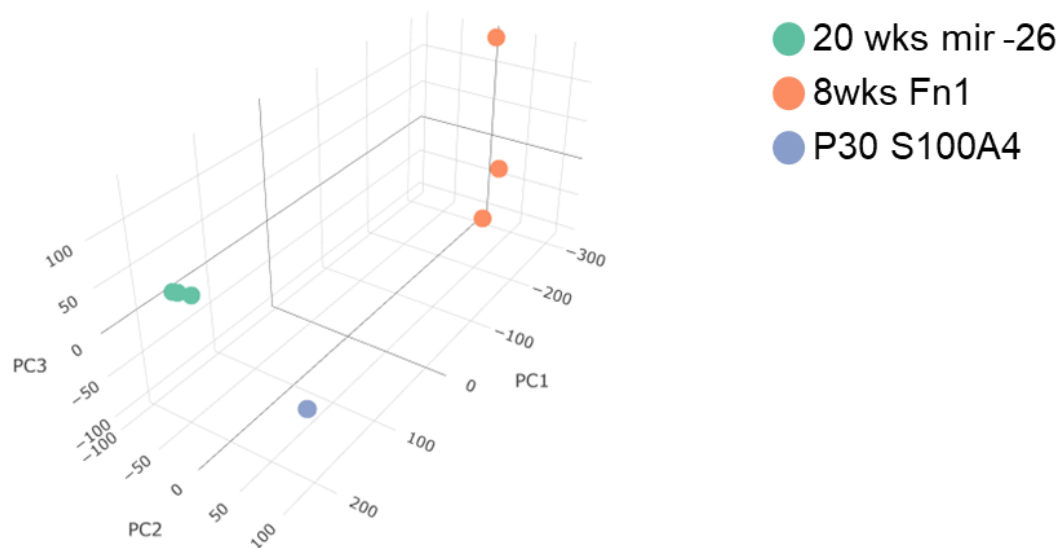


Figure 3.13 Clustering of adult lens control samples by 3-D PCA plot.

3.11 Differential expression analysis identifies widespread transcriptomic changes in adult lens Kos

Among the three developmental groups analyzed, the adult lens cKO datasets exhibited the most extensive differential gene expression. Using a p-value cutoff of 0.05 and a fold change $\geq |1.5|$, a total of 1,242 differentially expressed genes (DEGs) were identified, including 715 upregulated and 527 downregulated genes. Applying a more stringent cutoff based on adjusted p-value (FDR < 0.05), the analysis yielded 164

upregulated and 21 downregulated genes. These DEGs represent the most statistically robust transcriptional changes in the adult cKO lenses. The volcano plot shows the overall DEG landscape (Figure 3.14), with the top 40 most significantly misregulated genes labeled. Upregulated genes are marked in red and downregulated genes in blue.

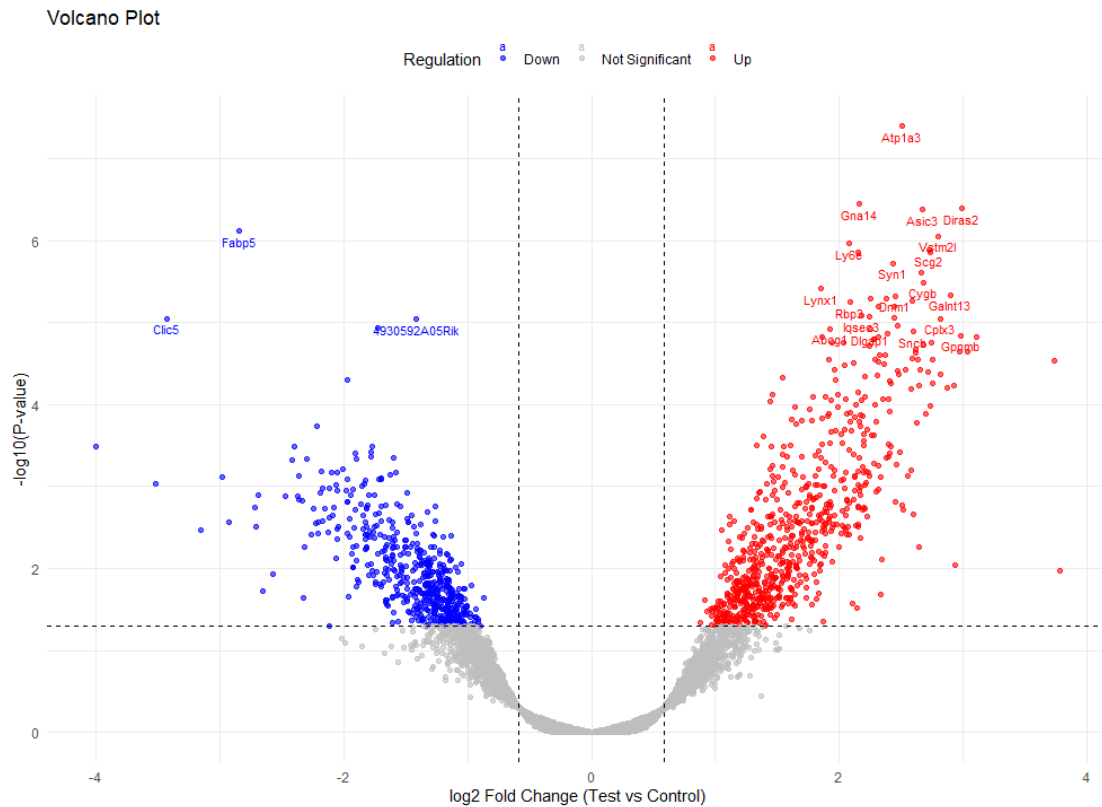


Figure 3.14 Volcano plot of DEGs in adult KO lenses. Log₂ fold change versus $-\log_{10}$ p-value. Red and blue dots represent significantly upregulated and downregulated genes, respectively ($\log_2\text{FC} \geq |0.58|$, p-value < 0.05). Labeled genes represent top 40 DEGs

The top 20 upregulated and 20 downregulated genes were selected based on the magnitude of their fold change and statistical significance. To evaluate their relevance to normal lens biology, I assessed each gene's expression and enrichment profile in wild-type (WT) lenses across developmental stages using iSyTE. Its expression and enrichment in wild-type (WT) lenses across developmental stages. The upregulated genes were generally lowly expressed in WT lens during development with only a few showing lens enriched expression, a pattern consistent with findings from the embryonic and early postnatal cKO groups (Figure 3.15). In contrast, many of the downregulated genes displayed strong expression and high enrichment in the WT lens (Figure 3.16), highlighting their likely importance in maintaining adult lens structure and function.

3.12 Gene ontology enrichment analysis of differentially expressed genes in adult lens KOs

For the upregulated DEGs, BP enrichment terms included “modulation of chemical synaptic transmission,” “transmembrane transport of inorganic ions,” and “sensory perception of light stimulus”. The latter is driven by abnormal expression of known retinal genes such as *Prph2*, *Rorb*, and *Crx*. The MF terms for the upregulated genes were dominated by various types of ion channel activity and transmembrane transporter activity, However, the downregulated DEGs were significantly enriched for lens-specific developmental and structural terms. BP categories included “eye development,” “camera-type eye development,” “lens development in camera-type eye,” and “epithelial cell differentiation.” MF terms for the downregulated genes featured “structural molecule activity,” “structural constituent of ribosome,” and “structural constituent of eye lens” (Figure 3.17A-D)

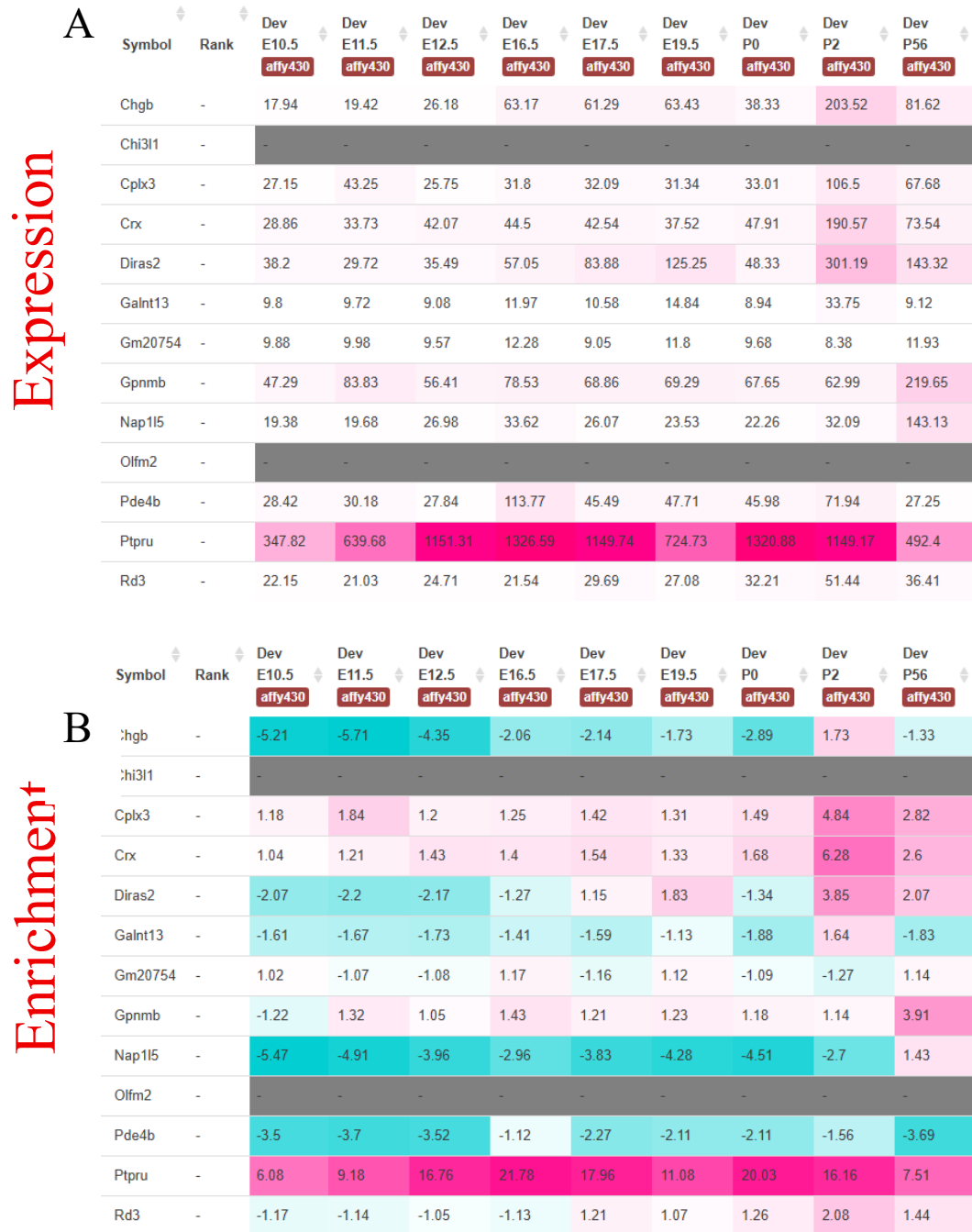


Figure 3.15 iSyTE analysis of upregulated DEGs from adult KO lenses (A) Expression and (B) lens enrichment patterns for upregulated DEGs across mouse lens developmental stages.

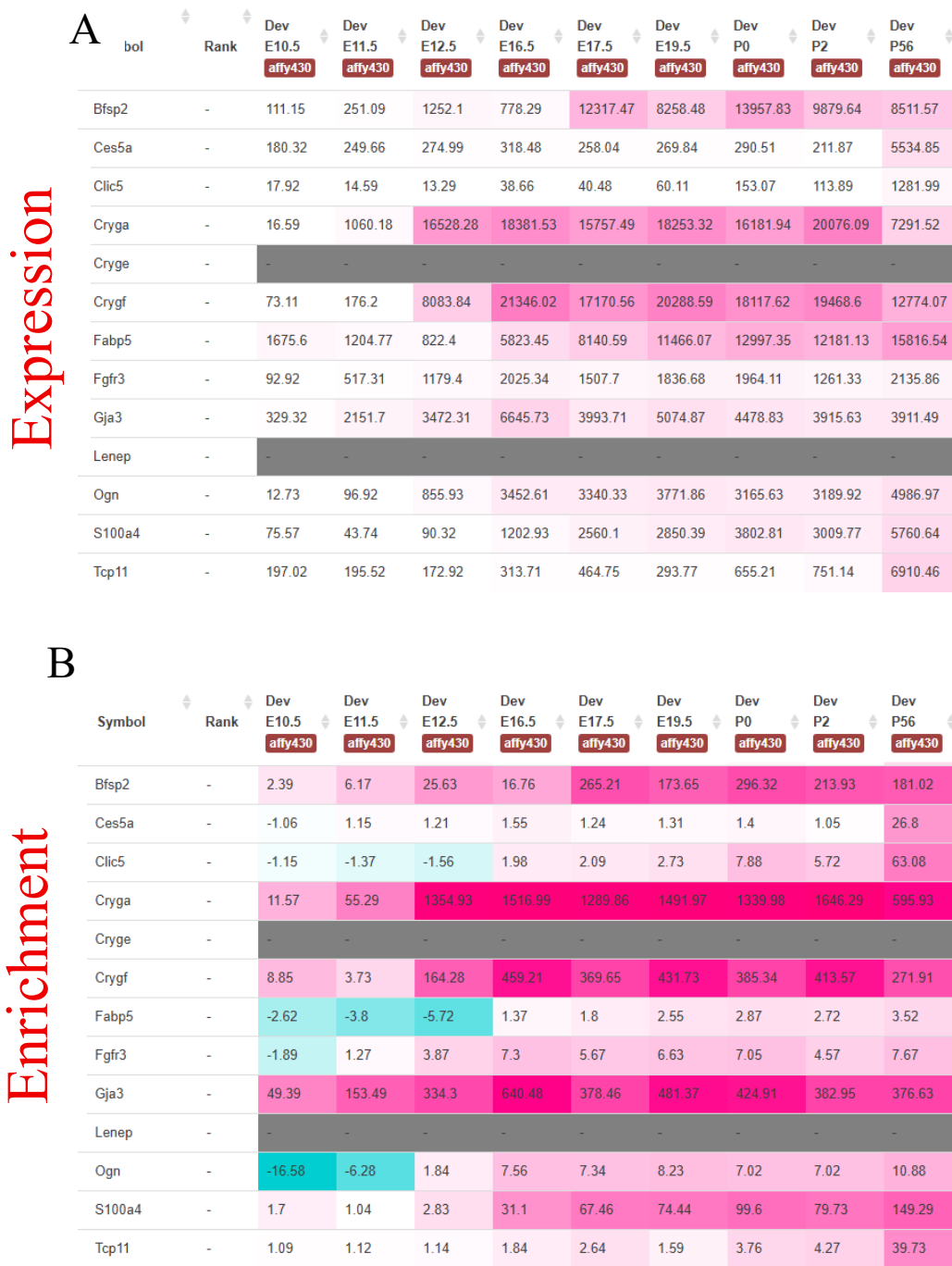
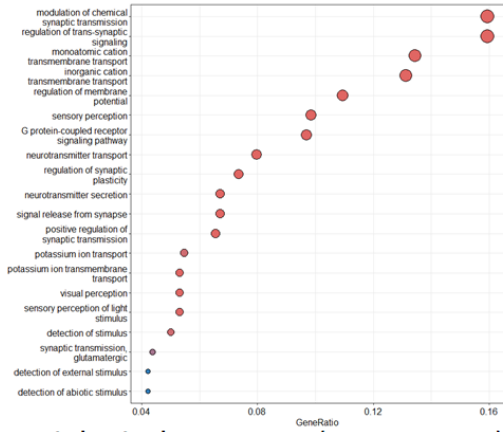
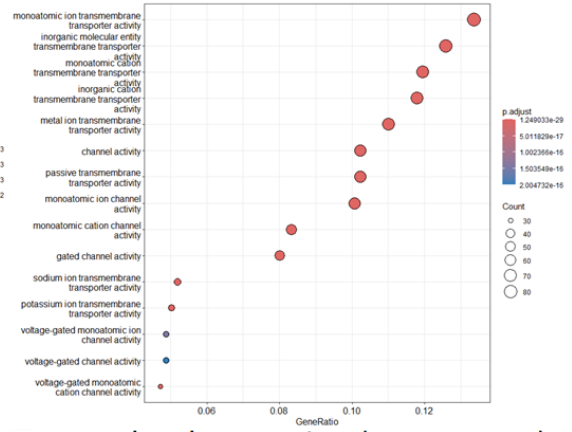


Figure 3.16 iSyTE analysis of downregulated DEGs from adult KO lenses (A) Expression and (B) lens enrichment patterns for downregulated DEGs across mouse lens developmental stages.

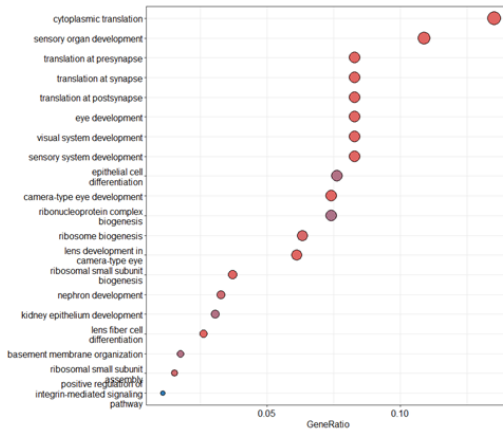
A. Biological Processes (Up genes)



B. Molecular Function (Up genes)



C. Biological Processes (Down genes)



D. Molecular Function (Down genes)

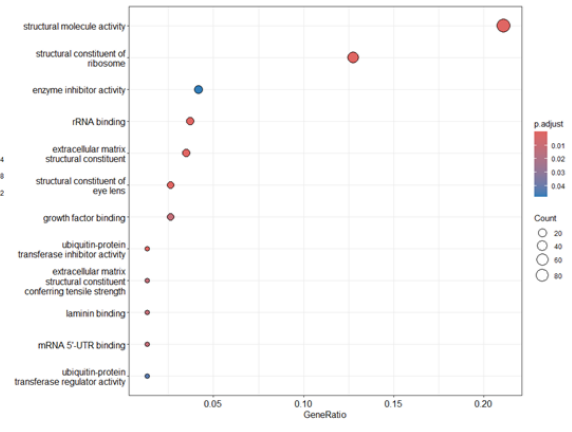


Figure 3.17 GO enrichment dot plots for upregulated and down regulated DEGs. (A) BP terms for upregulated genes. (B) MF terms for upregulated genes. (C) BP terms for downregulated genes (D) MF terms for downregulated genes

Chapter 4

DISCUSSION

A comprehensive meta-analysis – on an unprecedented level – of lens transcriptome datasets from stages representative of embryonic, early postnatal, and adult ages was performed. The embryonic and adult lens cKO meta-analysis reveals GO terms "visual system development," "eye development," and "lens development in camera-type eye" as significantly enriched in the downregulated gene set as strongly indicating that the meta-analysis successfully captured biologically relevant disruptions common to lens development and biology. These enriched terms were driven by multiple key lens genes including *Crygf*, *Crygb*, *Dnase2b*, and *Bfsp1* that were downregulated across the embryonic cKO datasets and in the adult cKO datasets, key genes such as *Cryg1*, *Gja3*, *Bfsp2*, *Dnase2b*, and *Fgfr3*. This reinforces the relevance of these genes as shared markers of lens dysregulation across developmental stages.

Among all developmental stages, only the embryonic cKO group showed enrichment for the term "lens fiber cell development" in GO analysis of downregulated genes. This is particularly significant, as lens fiber cells make up the bulk of the lens mass and are essential for its optical clarity and structural integrity. The disruption of this process implies that distinct gene perturbations during embryonic stages may ultimately impair the differentiation and maturation of these specialized cells. Supporting this, iSyTE analysis of the top 20 downregulated genes revealed that all were highly expressed and lens-enriched during embryonic stages. Moreover, comparative analysis with the iSyTE Lens Epithelium (Epi) vs Fiber Cells (Fib) cell-type specific

transcriptome data shows that these genes are more highly expressed in fibers indicating their likely requirement for normal lens fiber cell development. Consistent downregulation across multiple cKO models suggests that these genes may represent a regulatory module essential for embryonic lens integrity, and possibly key to lens pathology.

Furthermore, several of these downregulated genes are well-established in lens biology. For example, *Crygf* and *Crygb* encode structural γ -crystallins critical for lens transparency and refraction. *Bfsp1* encodes a lens-specific intermediate filament protein essential for maintaining fiber cell organization, and *Dnase2b* is a known effector of nuclear degradation during fiber cell terminal differentiation. Importantly, the meta-analysis also identified novel candidate genes not previously investigated in the lens but showing strong downregulation and high fiber-cell enrichment, such as *Tmprss11e*, *Ermap*, *Uox*, and *Myo7b*. *Tmprss11e*, a serine protease, shows a sharp increase in its gene expression at E14.5 in normal lenses and is more highly expressed in fiber cells than epithelial cells. *Ermap* (erythroblast membrane-associated protein) is a transmembrane protein which is also highly expressed in the lens. *Uox*, (urate oxidase) though moderately expressed, is highly enriched in fiber cells and could play a previously unrecognized role in lens metabolism or oxidative stress regulation. *Myo7b*, a cytoskeletal regulator, stands out as a promising candidate due to its putative role in cell shape and organization. Given that other myosin family members, such as *Myh9* (NMIIA) (Islam et al., 2023), have been implicated in epithelial cell alignment during fiber cell formation and differentiation, *Myo7b* may also contribute to cytoskeletal remodeling during lens development and warrants further investigation.

Conversely, upregulated DEGs in the embryonic cKOs were associated with GO terms that are not lens-specific, including “muscle cell differentiation,” “response to wounding,” “regulation of system process,” “skin development,” and “osteoblast differentiation.” These terms likely reflect the abnormal activation of non-lens transcriptional programs that are normally repressed in lens cells. This may be due to de-repression caused by the loss of key developmental regulators, compensatory responses to gene knockout, or generalized cellular stress and inflammatory signaling. Regardless of the precise mechanism, the enrichment of non-lens biological processes suggests a possible loss of lens identity (which may be to varying extents) and abnormal lens transcriptome across embryonic knockout lenses.

The meta-analysis of postnatal lens cKO datasets yielded the fewest significantly differentially expressed genes among all the developmental stages analyzed. Nonetheless, the 13 upregulated genes identified in this group were sufficient to yield enriched Gene Ontology (GO) terms through DAVID analysis including "visual perception," "retina development in camera-type eye," and "positive regulation of apoptotic process." Unlike in the embryonic lens datasets where these terms were driven by the downregulation of lens-enriched genes, the postnatal enrichment of “visual perception” was due to the upregulation of retina-specific genes, including *Prph2*, *Pdc*, *Pde6b*, and *Sag*. These genes are canonically involved in retina photoreceptor structure and function (Sullivan et al., 2017; Tebbe et al., 2022; Thulin et al., 1999; Zhang & Cote, 2005). This finding suggests that there are mechanisms in the lens to ensure that retinal gene expression is normally repressed during lens development, and even in the postnatal stages. The upregulation of such genes in postnatal cKOs also implies that perturbation of specific genes/regulatory pathways can lift away these repressive

controls, potentially compromising lens identity or triggering ectopic transcriptional activity. Recent reports offer independent support to there being mechanisms in place in the lens to repress neural and retinal gene expression (Maddala et al., 2021; Tangeman et al., 2024).

In the adult lens cKO meta-analysis, we observed a pronounced upregulation of retinal-specific genes, including *Crx*, *Rd3*, *Pde4b*, and *Cplx3*, consistent with findings from the postnatal dataset and further supporting the notion that retinal gene programs are aberrantly activated in the lens under conditions of gene disruption. Concurrently, downregulated genes were significantly enriched for lens-relevant Gene Ontology (GO) terms such as "eye development," "lens development in camera-type eye," and "epithelial cell differentiation," also underscoring the continued importance of these regulatory programs for lens integrity even in adulthood. A particularly noteworthy feature of the adult lens transcriptomic response was the marked enrichment of GO terms related to "ion channel activity" and "transmembrane transporter activity" among upregulated genes. The adult lens relies heavily on tissue maintenance, ionic and metabolic homeostasis regulation to preserve transparency and function (Donaldson et al., 2017; Mathias et al., 2010). The observed upregulation of ion transport-related genes likely reflects compensatory mechanisms triggered by disruption of ionic balance, which is critical for preventing osmotic stress, protein aggregation, and fiber cell disorganization. This response suggests that critical gene perturbations in adult cKOs compromise the fine-tuned ionic microenvironment of the lens, prompting transcriptional adjustments to preserve homeostasis. Taken together, these findings indicate that lens pathology in adult cKOs is strongly linked to the breakdown of

homeostatic control, as evidenced by the activation of stress-response pathways and the loss of lens-specific gene expression signatures.

In conclusion, this comprehensive meta-analysis of lens transcriptome has led to the recognition of a gene set underlying lens defects, commonly mis-regulated in different mouse gene-perturbation models. These data advance our understanding of the common pathways associated with lens pathology and inform on new targets that can be considered in therapeutic approaches for cataract.

Chapter 5

FUTURE DIRECTIONS

While this stage-classified meta-analysis of lens KO RNA-seq datasets has uncovered a set of misregulated genes associated with lens pathology, some caveats must be acknowledged. First, differential expression analysis (DEA) was conducted on pooled datasets within each developmental stage group. Although this approach enhances statistical power and enables the detection of shared transcriptional signatures, it may obscure study-specific effects and over-represent genes that are differentially expressed in only a subset of the datasets. Therefore, future work should include independent DEA of each dataset to determine whether the identified gene set is consistently and significantly misregulated across individual studies, thereby validating their biological relevance and robustness.

Additionally, while batch normalization was performed using laboratory group as covariate, other confounding variables such as mouse strain, genetic background, and sex were not explicitly modeled. Future analyses should aim to systematically incorporate metadata. Furthermore, in future studies, curating datasets based on phenotypic severity—including only KOs with documented lens abnormalities—could enhance the sensitivity for identifying critical misregulated pathways.

Finally, while the current meta-analysis was stage-stratified, future efforts could benefit from cross-stage integrative clustering of KO samples to determine whether transcriptomic similarity better reflects phenotypic outcomes than developmental timing alone.

REFERENCES

- Aryal, S., Anand, D., Hernandez, F. G., Weatherbee, B. A. T., Huang, H., Reddy, A. P., Wilmarth, P. A., David, L. L., & Lachke, S. A. (2020). MS/MS in silico subtraction-based proteomic profiling as an approach to facilitate disease gene discovery: Application to lens development and cataract. *Human Genetics*, *139*(2), 151–184. <https://doi.org/10.1007/s00439-019-02095-5>
- Bassnett, S. (2002). Lens Organelle Degradation. *Experimental Eye Research*, *74*(1), 1–6. <https://doi.org/10.1006/exer.2001.1111>
- Bell, S. J., Oluonye, N., Harding, P., & Moosajee, M. (2020). Congenital cataract: A guide to genetic and clinical management. *Therapeutic Advances in Rare Disease*, *1*, 2633004020938061. <https://doi.org/10.1177/2633004020938061>
- Bhat, S. P. (2001). The ocular lens epithelium. *Bioscience Reports*, *21*(4), 537–563. <https://doi.org/10.1023/a:1017952128502>
- Blixt, A., Landgren, H., Johansson, B. R., & Carlsson, P. (2007). Foxe3 is required for morphogenesis and differentiation of the anterior segment of the eye and is sensitive to Pax6 gene dosage. *Developmental Biology*, *302*(1), 218–229. <https://doi.org/10.1016/j.ydbio.2006.09.021>

- Cicinelli, M. V., Buchan, J. C., Nicholson, M., Varadaraj, V., & Khanna, R. C. (2023). Cataracts. *The Lancet*, *401*(10374), 377–389. [https://doi.org/10.1016/S0140-6736\(22\)01839-6](https://doi.org/10.1016/S0140-6736(22)01839-6)
- Coomson, S. Y., & Lachke, S. A. (2025). Bringing signaling complexity into focus. *eLife*, *14*, e106519. <https://doi.org/10.7554/eLife.106519>
- Cvekl, A., & Zhang, X. (2017). Signaling and gene regulatory networks in mammalian lens development. *Trends in Genetics : TIG*, *33*(10), 677–702. <https://doi.org/10.1016/j.tig.2017.08.001>
- Dash, S., Brastrom, L. K., Patel, S. D., Scott, C. A., Slusarski, D. C., & Lachke, S. A. (2020a). The master transcription factor SOX2, mutated in anophthalmia/microphthalmia, is post-transcriptionally regulated by the conserved RNA-binding protein RBM24 in vertebrate eye development. *Human Molecular Genetics*, *29*(4), 591–604. <https://doi.org/10.1093/hmg/ddz278>
- Dash, S., Brastrom, L. K., Patel, S. D., Scott, C. A., Slusarski, D. C., & Lachke, S. A. (2020b). The master transcription factor SOX2, mutated in anophthalmia/microphthalmia, is post-transcriptionally regulated by the conserved RNA-binding protein RBM24 in vertebrate eye development. *Human Molecular Genetics*, *29*(4), 591–604. <https://doi.org/10.1093/hmg/ddz278>
- Dash, S., Dang, C. A., Beebe, D. C., & Lachke, S. A. (2015). Deficiency of the RNA binding protein Caprin2 causes lens defects and features of Peters anomaly.

Developmental Dynamics : An Official Publication of the American Association of Anatomists, 244(10), 1313–1327.

<https://doi.org/10.1002/dvdy.24303>

Dash, S., Siddam, A. D., Barnum, C. E., Janga, S. C., & Lachke, S. A. (2016). RNA-binding proteins in eye development and disease: Implication of conserved RNA granule components. *WIREs RNA*, 7(4), 527–557.

<https://doi.org/10.1002/wrna.1355>

Disatham, J., Chauss, D., Gheyas, R., Brennan, L., Blanco, D., Daley, L., Menko, A. S., & Kantorow, M. (2019). Lens differentiation is characterized by stage-specific changes in chromatin accessibility correlating with differentiation state-specific gene expression. *Developmental Biology*, 453(1), 86–104.

<https://doi.org/10.1016/j.ydbio.2019.04.020>

Donaldson, P. J., Grey, A. C., Maceo Heilman, B., Lim, J. C., & Vaghefi, E. (2017). The physiological optics of the lens. *Progress in Retinal and Eye Research*, 56, e1–e24. <https://doi.org/10.1016/j.preteyeres.2016.09.002>

Faber, S. C., Robinson, M. L., Makarenkova, H. P., & Lang, R. A. (2002). Bmp signaling is required for development of primary lens fiber cells. *Development*, 129(15), 3727–3737. <https://doi.org/10.1242/dev.129.15.3727>

Fujimoto, M., Izu, H., Seki, K., Fukuda, K., Nishida, T., Yamada, S., Kato, K., Yonemura, S., Inouye, S., & Nakai, A. (2004). HSF4 is required for normal cell growth and differentiation during mouse lens development. *The EMBO Journal*, 23(21), 4297–4306. <https://doi.org/10.1038/sj.emboj.7600435>

- Gong, X., Cheng, C., & Xia, C. (2007). Connexins in lens development and cataractogenesis. *The Journal of Membrane Biology*, 218(1–3), 9–12.
<https://doi.org/10.1007/s00232-007-9033-0>
- Graw, J. (2010). Eye development. *Current Topics in Developmental Biology*, 90, 343–386. [https://doi.org/10.1016/S0070-2153\(10\)90010-0](https://doi.org/10.1016/S0070-2153(10)90010-0)
- Gupta, P., Gurnani, B., & Patel, B. C. (2025). Pediatric Cataract. In *StatPearls*. StatPearls Publishing. <http://www.ncbi.nlm.nih.gov/books/NBK572080/>
- Harding, P., & Moosajee, M. (2019a). The Molecular Basis of Human Anophthalmia and Microphthalmia. *Journal of Developmental Biology*, 7(3), 16.
<https://doi.org/10.3390/jdb7030016>
- Harding, P., & Moosajee, M. (2019b). The Molecular Basis of Human Anophthalmia and Microphthalmia. *Journal of Developmental Biology*, 7(3), 16.
<https://doi.org/10.3390/jdb7030016>
- Hejtmancik, J. F., & Kantorow, M. (2004). Molecular genetics of age-related cataract. *Experimental Eye Research*, 79(1), 3–9.
<https://doi.org/10.1016/j.exer.2004.03.014>
- Horwitz, J. (2003). Alpha-crystallin. *Experimental Eye Research*, 76(2), 145–153.
[https://doi.org/10.1016/S0014-4835\(02\)00278-6](https://doi.org/10.1016/S0014-4835(02)00278-6)
- Islam, S. T., Cheng, C., Parreno, J., & Fowler, V. M. (2023). Nonmuscle Myosin IIA Regulates the Precise Alignment of Hexagonal Eye Lens Epithelial Cells During Fiber Cell Formation and Differentiation. *Investigative Ophthalmology & Visual Science*, 64(4), 20. <https://doi.org/10.1167/iovs.64.4.20>

- Ivanescu, A., Popescu, S., Gaita, L., Albai, O., Braha, A., & Timar, R. (2024). Risk Factors for Cataracts in Patients with Diabetes Mellitus. *Journal of Clinical Medicine*, *13*(23), 7005. <https://doi.org/10.3390/jcm13237005>
- Kakrana, A., Yang, A., Anand, D., Djordjevic, D., Ramachandruni, D., Singh, A., Huang, H., Ho, J. W. K., & Lachke, S. A. (2018). iSyTE 2.0: A database for expression-based gene discovery in the eye. *Nucleic Acids Research*, *46*(D1), D875–D885. <https://doi.org/10.1093/nar/gkx837>
- Khokhar, S., Pillay, G., & Agarwal, E. (2018). Pediatric Cataract—Importance of Early Detection and Management. *Indian Journal of Pediatrics*, *85*(3), 209–216. <https://doi.org/10.1007/s12098-017-2482-2>
- Kim, J. I., Li, T., Ho, I.-C., Grusby, M. J., & Glimcher, L. H. (1999). Requirement for the c-Maf transcription factor in crystallin gene regulation and lens development. *Proceedings of the National Academy of Sciences of the United States of America*, *96*(7), 3781–3785. <https://doi.org/10.1073/pnas.96.7.3781>
- Klemenz, R., Fröhli, E., Aoyama, A., Hoffmann, S., Simpson, R. J., Moritz, R. L., & Schäfer, R. (1991). Alpha B crystallin accumulation is a specific response to Ha-ras and v-mos oncogene expression in mouse NIH 3T3 fibroblasts. *Molecular and Cellular Biology*, *11*(2), 803–812. <https://doi.org/10.1128/mcb.11.2.803-812.1991>
- Kuszak, J. R., Zoltoski, R. K., & Sivertson, C. (2004). Fibre cell organization in crystalline lenses. *Experimental Eye Research*, *78*(3), 673–687. <https://doi.org/10.1016/j.exer.2003.09.016>

- Lachke, S. A. (2022). RNA-binding proteins and post-transcriptional regulation in lens biology and cataract: Mediating spatiotemporal expression of key factors that control the cell cycle, transcription, cytoskeleton and transparency. *Experimental Eye Research*, 214, 108889. <https://doi.org/10.1016/j.exer.2021.108889>
- Lachke, S. A., Alkuraya, F. S., Kneeland, S. C., Ohn, T., Aboukhalil, A., Howell, G. R., Saadi, I., Cavallusco, R., Yue, Y., Tsai, A. C.-H., Nair, K. S., Cosma, M. I., Smith, R. S., Hodges, E., AlFadhli, S. M., Al-Hajeri, A., Shamseldin, H. E., Behbehani, A., Hannon, G. J., ... Maas, R. L. (2011). Mutations in the RNA Granule Component TDRD7 Cause Cataract and Glaucoma. *Science (New York, N.y.)*, 331(6024), 1571–1576. <https://doi.org/10.1126/science.1195970>
- Lachke, S. A., Ho, J. W. K., Kryukov, G. V., O’Connell, D. J., Aboukhalil, A., Bulyk, M. L., Park, P. J., & Maas, R. L. (2012). iSyTE: Integrated Systems Tool for Eye gene discovery. *Investigative Ophthalmology & Visual Science*, 53(3), 1617–1627. <https://doi.org/10.1167/iovs.11-8839>
- Lachke, S. A., & Maas, R. L. (2010a). Building the developmental oculome: Systems biology in vertebrate eye development and disease. *WIREs Systems Biology and Medicine*, 2(3), 305–323. <https://doi.org/10.1002/wsbm.59>
- Lachke, S. A., & Maas, R. L. (2010b). Building the Developmental Oculome: Vertebrate Eye Development and Disease. *Wiley Interdisciplinary Reviews. Systems Biology and Medicine*, 2(3), 305–323. <https://doi.org/10.1002/wsbm.59>

- Land, M. F. (2012). The evolution of lenses. *Ophthalmic & Physiological Optics: The Journal of the British College of Ophthalmic Opticians (Optometrists)*, 32(6), 449–460. <https://doi.org/10.1111/j.1475-1313.2012.00941.x>
- Li, J., Chen, X., Yan, Y., & Yao, K. (2020). Molecular genetics of congenital cataracts. *Experimental Eye Research*, 191, 107872. <https://doi.org/10.1016/j.exer.2019.107872>
- Liu, W., Lagutin, O. V., Mende, M., Streit, A., & Oliver, G. (2006). Six3 activation of Pax6 expression is essential for mammalian lens induction and specification. *The EMBO Journal*, 25(22), 5383–5395. <https://doi.org/10.1038/sj.emboj.7601398>
- Maddala, R., Gao, J., Mathias, R. T., Lewis, T. R., Arshavsky, V. Y., Levine, A., Backer, J. M., Bresnick, A. R., & Rao, P. V. (2021). Absence of S100A4 in the mouse lens induces an aberrant retina-specific differentiation program and cataract. *Scientific Reports*, 11(1), 2203. <https://doi.org/10.1038/s41598-021-81611-y>
- Mathias, R. T., White, T. W., & Gong, X. (2010). Lens Gap Junctions in Growth, Differentiation, and Homeostasis. *Physiological Reviews*, 90(1), 179–206. <https://doi.org/10.1152/physrev.00034.2009>
- McAvoy, J. W., Chamberlain, C. G., de Iongh, R. U., Hales, A. M., & Lovicu, F. J. (1999). Lens development. *Eye (London, England)*, 13 (Pt 3b), 425–437. <https://doi.org/10.1038/eye.1999.117>

- Moreau, K. L., & King, J. A. (2012). Protein Misfolding and Aggregation in Cataract Disease and Prospects for Prevention. *Trends in Molecular Medicine*, 18(5), 273–282. <https://doi.org/10.1016/j.molmed.2012.03.005>
- Moshirfar, M., Webster, C. R., Seitz, T. S., Ronquillo, Y. C., & Hoopes, P. C. (2022). Ocular Features and Clinical Approach to Cataract and Corneal Refractive Surgery in Patients with Myotonic Dystrophy. *Clinical Ophthalmology (Auckland, N.Z.)*, 16, 2837–2842. <https://doi.org/10.2147/OPHTH.S372633>
- Patel, S. D., Anand, D., Motohashi, H., Katsuoka, F., Yamamoto, M., & Lachke, S. A. (2022). Deficiency of the bZIP transcription factors Mafg and Mafk causes misexpression of genes in distinct pathways and results in lens embryonic developmental defects. *Frontiers in Cell and Developmental Biology*, 10, 981893. <https://doi.org/10.3389/fcell.2022.981893>
- Perng, M.-D., Zhang, Q., & Quinlan, R. A. (2007). Insights into the beaded filament of the eye lens. *Experimental Cell Research*, 313(10), 2180–2188. <https://doi.org/10.1016/j.yexcr.2007.04.005>
- Pollreisz, A., & Schmidt-Erfurth, U. (2010). Diabetic Cataract—Pathogenesis, Epidemiology and Treatment. *Journal of Ophthalmology*, 2010, 608751. <https://doi.org/10.1155/2010/608751>
- Pontoriero, G. F., Smith, A. N., Miller, L.-A. D., Radice, G. L., West-Mays, J. A., & Lang, R. A. (2009). Co-operative roles for E-cadherin and N-cadherin during lens vesicle separation and lens epithelial cell survival. *Developmental Biology*, 326(2), 403–417. <https://doi.org/10.1016/j.ydbio.2008.10.011>

- Rao, P. V. (2008). The pulling, pushing and fusing of lens fibers. *Cell Adhesion & Migration*, 2(3), 170–173. <https://doi.org/10.4161/cam.2.3.6495>
- Robinson, M. L. (2006). An Essential Role for FGF Receptor Signaling in Lens Development. *Seminars in Cell & Developmental Biology*, 17(6), 726–740. <https://doi.org/10.1016/j.semcdb.2006.10.002>
- Rong, P., Wang, X., Niesman, I., Wu, Y., Benedetti, L. E., Dunia, I., Levy, E., & Gong, X. (2002). Disruption of Gja8 (alpha8 connexin) in mice leads to microphthalmia associated with retardation of lens growth and lens fiber maturation. *Development (Cambridge, England)*, 129(1), 167–174. <https://doi.org/10.1242/dev.129.1.167>
- Shah, S. P., Taylor, A. E., Sowden, J. C., Ragge, N., Russell-Eggitt, I., Rahi, J. S., & Gilbert, C. E. (2012). Anophthalmos, Microphthalmos, and Coloboma in the United Kingdom: Clinical Features, Results of Investigations, and Early Management. *Ophthalmology*, 119(2), 362–368. <https://doi.org/10.1016/j.ophtha.2011.07.039>
- Sharma, K. K., & Santhoshkumar, P. (2009). Lens Aging: Effects of Crystallins. *Biochimica et Biophysica Acta*, 1790(10), 1095–1108. <https://doi.org/10.1016/j.bbagen.2009.05.008>
- Shiels, A., Bennett, T. M., & Hejtmancik, J. F. (2010). Cat-Map: Putting cataract on the map. *Molecular Vision*, 16, 2007–2015.

- Shiels, A., & Hejtmancik, J. F. (2017). Mutations and mechanisms in congenital and age-related cataracts. *Experimental Eye Research*, *156*, 95–102.
<https://doi.org/10.1016/j.exer.2016.06.011>
- Shiels, A., & Hejtmancik, J. F. (2021). Inherited Cataracts: Genetic Mechanisms and Pathways New and Old. *Experimental Eye Research*, *209*, 108662.
<https://doi.org/10.1016/j.exer.2021.108662>
- Siddam, A. D., Gautier-Courteille, C., Perez-Campos, L., Anand, D., Kakrana, A., Dang, C. A., Legagneux, V., Méreau, A., Viet, J., Gross, J. M., Paillard, L., & Lachke, S. A. (2018). The RNA-binding protein Celf1 post-transcriptionally regulates p27Kip1 and Dnase2b to control fiber cell nuclear degradation in lens development. *PLoS Genetics*, *14*(3), e1007278.
<https://doi.org/10.1371/journal.pgen.1007278>
- Slingsby, C., Wistow, G. J., & Clark, A. R. (2013). Evolution of crystallins for a role in the vertebrate eye lens. *Protein Science : A Publication of the Protein Society*, *22*(4), 367–380. <https://doi.org/10.1002/pro.2229>
- Smets, K. J., Barlow, T., & Vanhaesebrouck, P. (2006). Maternal vitamin A deficiency and neonatal microphthalmia: Complications of biliopancreatic diversion? *European Journal of Pediatrics*, *165*(7), 502–504.
<https://doi.org/10.1007/s00431-006-0120-5>
- Smith, A. N., Miller, L.-A., Radice, G., Ashery-Padan, R., & Lang, R. A. (2009). Stage-dependent modes of Pax6-Sox2 epistasis regulate lens development and

eye morphogenesis. *Development (Cambridge, England)*, 136(17), 2977–2985.

<https://doi.org/10.1242/dev.037341>

Sullivan, L. S., Bowne, S. J., Koboldt, D. C., Cadena, E. L., Heckenlively, J. R., Branham, K. E., Wheaton, D. H., Jones, K. D., Ruiz, R. S., Pennesi, M. E., Yang, P., Davis-Boozer, D., Northrup, H., Gurevich, V. V., Chen, R., Xu, M., Li, Y., Birch, D. G., & Daiger, S. P. (2017). A Novel Dominant Mutation in SAG, the Arrestin-1 Gene, Is a Common Cause of Retinitis Pigmentosa in Hispanic Families in the Southwestern United States. *Investigative Ophthalmology & Visual Science*, 58(5), 2774–2784.

<https://doi.org/10.1167/iovs.16-21341>

Tangeman, J. A., Rebull, S. M., Grajales-Esquivel, E., Weaver, J. M., Bendezu-Sayas, S., Robinson, M. L., Lachke, S. A., & Del Rio-Tsonis, K. (2024). Integrated single-cell multiomics uncovers foundational regulatory mechanisms of lens development and pathology. *Development (Cambridge, England)*, 151(1), dev202249. <https://doi.org/10.1242/dev.202249>

Tebbe, L., Sakthivel, H., Makia, M. S., Kakakhel, M., Conley, S. M., Al-Ubaidi, M. R., & Naash, M. I. (2022). Prph2 disease mutations lead to structural and functional defects in the RPE. *FASEB Journal : Official Publication of the Federation of American Societies for Experimental Biology*, 36(5), e22284. <https://doi.org/10.1096/fj.202101562RR>

- Thulin, C. D., Howes, K., Driscoll, C. D., Savage, J. R., Rand, T. A., Baehr, W., & Willardson, B. M. (1999). The immunolocalization and divergent roles of phosphodiesterase-3 and phosphodiesterase-3-like protein in the retina. *Molecular Vision*, 5, 40.
- Valleix, S., Niel, F., Nedelec, B., Algros, M.-P., Schwartz, C., Delbosc, B., Delpech, M., & Kantelip, B. (2006). Homozygous nonsense mutation in the FOXE3 gene as a cause of congenital primary aphakia in humans. *American Journal of Human Genetics*, 79(2), 358–364. <https://doi.org/10.1086/505654>
- Verma, A. S., & Fitzpatrick, D. R. (2007). Anophthalmia and microphthalmia. *Orphanet Journal of Rare Diseases*, 2, 47. <https://doi.org/10.1186/1750-1172-2-47>
- Wigle, J. T., Chowdhury, K., Gruss, P., & Oliver, G. (1999). Prox1 function is crucial for mouse lens-fibre elongation. *Nature Genetics*, 21(3), Article 3. <https://doi.org/10.1038/6844>
- Williamson, K. A., & FitzPatrick, D. R. (2014). The genetic architecture of microphthalmia, anophthalmia and coloboma. *European Journal of Medical Genetics*, 57(8), 369–380. <https://doi.org/10.1016/j.ejmg.2014.05.002>
- Wistow, G. (2012). The human crystallin gene families. *Human Genomics*, 6(1), 26. <https://doi.org/10.1186/1479-7364-6-26>
- Yang, Y., Stopka, T., Golestaneh, N., Wang, Y., Wu, K., Li, A., Chauhan, B. K., Gao, C. Y., Cveklová, K., Duncan, M. K., Pestell, R. G., Chepelinsky, A. B., Skoultchi, A. I., & Cvekl, A. (2006). Regulation of α A-crystallin via Pax6, c-

- Maf, CREB and a broad domain of lens-specific chromatin. *The EMBO Journal*, 25(10), 2107–2118. <https://doi.org/10.1038/sj.emboj.7601114>
- Yu, X., Zheng, H., Chan, M. T., & Wu, W. K. K. (2017). MicroRNAs: New players in cataract. *American Journal of Translational Research*, 9(9), 3896–3903.
- Zhang, X., & Cote, R. H. (2005). cGMP signaling in vertebrate retinal photoreceptor cells. *Frontiers in Bioscience: A Journal and Virtual Library*, 10, 1191–1204. <https://doi.org/10.2741/1612>